

AN ABSTRACT OF THE THESIS OF

Corina P. Mullen for the degree of Master of Science in Physics presented on December 13, 1996. Title: High-Temperature, High-Pressure NMR Probe for Superconducting Magnets

Abstract approved: _____
William W. Warren, Jr.

A high-temperature, high-pressure autoclave has been adapted for use with a high-field nuclear magnetic resonance spectrometer. The autoclave has an internal pressure range of atmospheric pressure to 1.5 kbar and a temperature range of 273 K to 1900 K. The autoclave is usable in a high field (8 T) magnet with a room-temperature, 76.4 mm bore. The autoclave was tested using assorted nuclear species with resonant frequencies ranging from 57 to 70 MHz at pressures ranging from atmospheric pressure to 1220 bar and temperatures ranging from 273 K to 448 K. Previously, the autoclave was used in conjunction with an iron magnet at temperatures to 1900 K and pressures to 1.5 kbar.

High-Temperature, High-Pressure NMR Probe for
Superconducting Magnets

by

Corina P. Mullen

A THESIS

submitted to

Oregon State University

in partial fulfillment of
the requirements for the
degree of

Master of Science

Presented December 13, 1996
Commencement June 1997

Master of Science thesis for Corina P. Mullen presented on
December 13, 1996

APPROVED:

Major Professor, representing Physics

Chair of Department of Physics

Redacted for Privacy

Dean of Graduate School

I understand that my thesis will become part of the
permanent collection of Oregon State University libraries.
My signature below authorizes release of my thesis to any
reader upon request.

Redacted for Privacy

Corina P. Mullen, Author

ACKNOWLEDGEMENTS

I would like to acknowledge the help and support of all the people who enabled me to complete this thesis. I would like to thank Dr. William W. Warren for his patience and for acting as my thesis advisor. I would like to thank Dr. John Gardner and Dr. Henri Jansen for acting as my thesis committee. I would also like to thank Dr. Philip Watson for acting as graduate council representative. In addition, I would like to acknowledge and thank the support staff at Oregon State University, especially in the departments of physics and chemistry, without whom the completion of this thesis would have been much more difficult.

I would like to thank my husband, James, and my daughters, Berlinnetta and Samantha, for their patience and support, especially when I was tired and irritable.

I would like to acknowledge the help of my professional colleagues, especially those who critiqued the final versions of the thesis.

Lastly, I would like to acknowledge the financial support of the United States Department of Education.

TABLE OF CONTENTS

	<u>Page</u>
INTRODUCTION	1
HISTORY	3
EXPERIMENTAL JUSTIFICATION	5
EXPERIMENTAL CONSTRUCTION	8
Water Cooling Channels	10
O-ring Adapter	12
Sample Cell and NMR Coil	14
Autoclave Support	23
RF Filters	23
EXPERIMENTAL PROCEDURE (CONSTRUCTION VERIFICATION) . .	31
CONCLUSION	53
BIBLIOGRAPHY	54

LIST OF FIGURES

<u>Figure</u>	<u>Page</u>
1. AgI Phase Diagram	7
2. Pressure vessel (autoclave) to be used in spectrometer with 76 mm bore.	9
3. Adapter to allow connection of interior and exterior liquid sample tubing through top of autoclave without loss of pressure.	13
4. Sample cell for use with liquid sample (Assembly Drawing).	15
5. Manufacturing drawing of delivery tube to be used with liquid samples.	16
6. Sample cell for use with liquid samples.	17
7. Cap for sample cell to be used with liquid samples.	18
8. Tuning and matching circuit to allow resonant frequencies of 57 to 70 MHz.	22
9. Mount to hold autoclave in the correct position with respect to the spectrometer.	24
10. Top view of autoclave support.	25

List of Figures (Continued)

<u>Figure</u>	<u>Page</u>
11. Bottom view of autoclave support.	26
12. Bottom view of autoclave mount.	27
13. Side view of autoclave mount.	28
14. RF Filters (Lunar Lander)	30
15. Liquid Hg spectrum gathered at RTP (Hg Spectrum #1). 33	
16. Liquid Hg spectrum gathered at RTP (Hg Spectrum #2). 34	
17. Liquid Hg spectrum gathered at RTP (Hg Spectrum #3). 35	
18. AgI powder at RTP before elevating pressure. . . .	36
19. AgI powder at 200 Bar	37
20. AgI powder at 400 Bar	38
21. AgI powder at 600 Bar.	39
22. AgI powder at 800 Bar.	40
23. AgI powder at 1000 Bar.	41

List of Figures (Continued)

<u>Figure</u>	<u>Page</u>
24. AgI powder at 1100 Bar.	43
25. AgI crystal at RTP before heating	44
26. AgI crystal at atmospheric pressure during heating from room temperature to 349 K.	45
27. AgI crystal at atmospheric pressure heating from 353 K to 356 K.	46
28. AgI crystal at atmospheric pressure during heating from 389 K to 399 K.	47
29. AgI crystal at atmospheric pressure and 407 K. . .	48
30. AgI crystal at atmospheric pressure and 431 K. . .	49
31. AgI crystal at atmospheric pressure heating from 433 K to 448 K.	51
32. AgI crystal at atmospheric pressure after heating while cooling from 308 K to 297 K.	52

High-Temperature, High-Pressure NMR Probe for Superconducting Magnets

INTRODUCTION

Many interesting phenomena may be studied using high-pressure, high-temperature nuclear magnetic resonance spectroscopy (NMR). For example, as mercury is heated under pressure to conditions near the liquid-vapor critical point ($T_c = 1760$ K, $P_c = 1510$ Bar), the density changes smoothly as does the conductivity (Schönherr, Schmutzler, and Hensel, 1979); however, at a point near, but not at, the liquid-vapor critical point, the ^{199}Hg Knight Shift, which is the shift in the resonance frequency of a nucleus placed in a magnetic field due to the interaction of the magnetic moment of the electron and the magnetic moment of the nucleus, changes abruptly (El-Hanany and Warren, 1975). By varying temperatures at elevated pressures, Knight Shift changes in cesium (^{133}Cs) may also be observed (Warren, Brennert, and El-Hanany, 1989).

There have been minifurnaces designed for use in NMR with ranges of 300 - 1875 K (Shaham, 1979). There are also probes for use at temperatures to 1200 °C for use with silicate melts (Shimokawa et al, 1990). However, with many standard NMR probes, conditions are limited to either moderately elevated temperatures or, in some cases, elevated pressures. While each of these conditions yields many interesting results, the study of some phenomena requires both elevated temperatures and elevated pressures.

Historically, high-temperature, high-pressure NMR has been conducted using low-field iron magnets; however, with the advent of NMR systems utilizing superconducting magnets, interest in high-field, high-temperature, high-pressure NMR has increased. With a magnetic field of 8 Tesla, many of the problems that plagued early high-temperature, high-pressure NMR experiments can be overcome, but with these benefits come unique experimental challenges due to the geometry and size constraints of the new NMR systems. Ploumbidis outlines some of the experimental challenges that occur in the design of a high-temperature, high-field NMR probe (1979).

HISTORY

High-pressure NMR is a well-known technique for studying phenomena that are related to density variations. However, much of the high-pressure NMR work has been performed at relatively low temperatures. Since nuclear resonance experiments can be performed at pressures above 50,000 bars, it is necessary to define what will be termed high-pressure (Benedek, 1963); for the purpose of this work, high-pressure will be limited to pressures below 1.5 kbar.

High-temperature NMR has been used for many decades to study a plethora of phenomena. For example, the coal liquefaction process has been observed, the structure and dynamics in zeolites have been studied, the structural mobility of silicate liquids has been explored (Stebbins and Farnan, 1989), electrical conductivity in ionic conductors has been studied, and defects in ionic crystals have been studied (Stebbins, 1991). High-temperature NMR has allowed the study of phase transitions in silicate glasses and liquids (Stebbins, 1992). Each of these applications may require a unique NMR probe and sample chamber. For instance, Aurora and Day have developed an high temperature probe for use with solid electrolytes. This probe has an evacuated sample cell to prevent the oxidation of the sample (Aurora and Day, 1982). A variable temperature probe that allows the regulation of oxygen partial pressure was designed by Kolem et al (1990). The list of experimental interests, and the probes necessary to study them, is endless.

The combination of elevated temperatures and elevated pressures has made possible observations of many interesting phenomena, such as metal to non-metal transitions. Some of the most notable experiments using high-temperature, high-pressure NMR were studies of the electronic structure of expanded liquid cesium (Warren, Brennert, and El-Hanany, 1989) and of the Knight Shift in expanded-liquid mercury (Warren and Hensel, 1982).

Each of these NMR applications introduces new design challenges. Probe designers must be aware of a multitude of potential problems ranging from the obvious concerns of magnetic materials to interactions between samples and sample cells. In addition, liquid samples present the opportunity to design viable containment methods which allow expansion (Sawyer and Gale, 1973). Stainless steel that is advertised as non-magnetic may, in actuality, be magnetic at high fields. Ceramics may become conducting at high temperatures. Adhesives may disintegrate at relatively low temperatures; other adhesives may contain particles of ferrous metal. The probe designer must become familiar with metals, ceramics, adhesives, electronics, and the proposed samples.

EXPERIMENTAL JUSTIFICATION

When the original mercury and cesium studies were performed, the autoclave was used in a two-Tesla iron magnet. Using conventional pulsed NMR techniques at a frequency of 13.2 MHz for ^{199}Hg , a signal-to-noise ratio of four was achieved with four hour data collection periods (El-Hanany and Warren, 1975). With an eight-Tesla field, a signal-to-noise ratio 16 times better than the signal-to-noise ratio in the two-Tesla field is theoretically possible. This means in an eight-Tesla field, a spectrum obtained in a 2 T field and signal averaged for 32 minutes can be achieved in less than 7.5 seconds. In practice, other considerations, such as skin depth in metallic samples, will contribute to the signal-to-noise ratio.

The autoclave was originally designed for the study of expanded liquid metals at temperatures near the liquid-vapor critical point. However, for the purpose of probe development, it was decided to test the autoclave in the high-field spectrometer using AgI crystals. To avoid the complications of liquid samples, silver iodide crystals were chosen as test material. For example, the use of crystals eliminated the need for a sealed, pressure-balanced sample cell. The frequency of AgI, 68 MHz, was within the range of the tuning circuit that had been designed for use with mercury. Silver iodide undergoes separate phase transitions at increased temperature and at increased pressure allowing both temperature and pressure performance of the autoclave to be tested (Mellander,

Bowling, and Baranowski, 1980). Figure 1 displays an AgI phase diagram based on the data gathered by Mellander et al (1980). In addition, silver iodide crystals were available.

At RTP, AgI is a mixture of β and γ phases. The more stable β phase is a hexagonal wurtzite structure, while the γ phase has the structure of cubic zincblende (Keen, 1993). At increased temperatures, AgI experiences a first-order phase transition to the fast-ionic α phase; the α phase is a body-centered cubic arrangement of I^- ions with a collection of Ag^+ ions that tend to occupy tetrahedral sites (Keen, 1993). This α phase is stable between 420 K and 828 K (Mellander, 1982). However, if the pressure is increased while the temperature of the AgI is above ~ 310 K, the mixed β/γ phase transforms to a rocksalt structure (Keen, 1993). There is an intermediate phase which is stable within a small temperature and pressure range. The approximate pressure extrema of this intermediate phase are 2.5 kbar and 4.2 kbar at 273 K; the approximate upper temperature extremum is 313 K at 3.3 kbar (Mellander, 1982).

The study of phase transitions in AgI is interesting in itself due to the effect of AgI content on the conductivity of certain superionic conducting glasses (Saito, 1996). While the AgI used to test the autoclave was crystalline, the apparatus could accommodate a glass sample with little, or no modification.

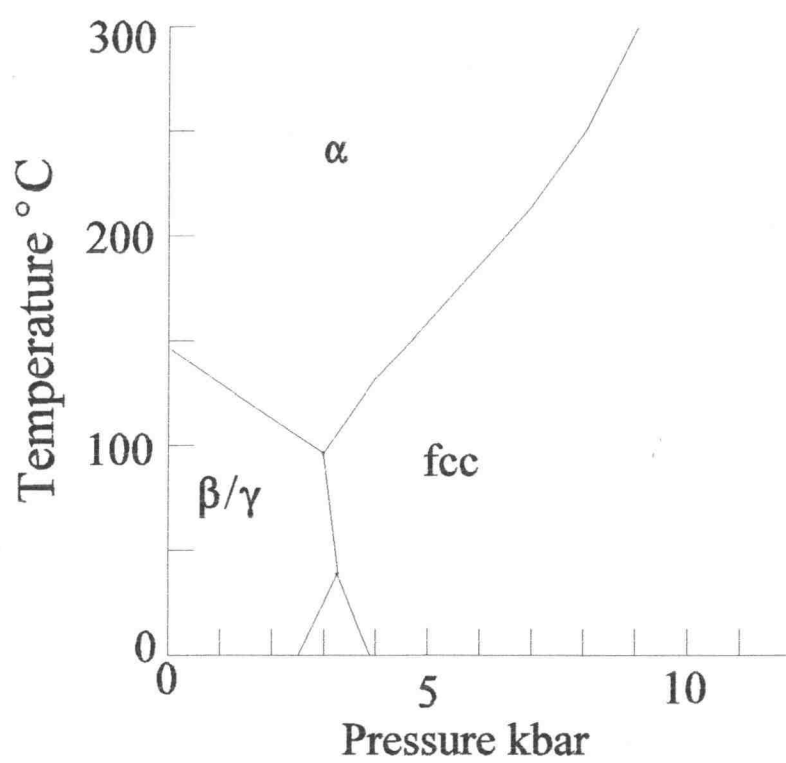


Figure 1 AgI Phase Diagram

EXPERIMENTAL CONSTRUCTION

Originally, the autoclave was designed to be used in an iron-core electromagnet with a 76.2 mm face separation. In order to fit into this magnet, the autoclave was constructed with an outer diameter of 75 mm; however, due to the design of the iron magnet, portions of the autoclave system that extended past the 9 inch diameter magnet faces could have a larger diameter than 76.2 mm. For example, the water for cooling was introduced into the autoclave via Swagelock[®] fittings that were soldered onto a ring which fit around the autoclave. Another appendage that increased the diameter of the autoclave outside the vicinity of the magnet faces was a set of RF filters for the heater and thermocouples. It was decided to adapt the autoclave for use with a superconducting magnet. The magnet was selected with a 76.2 mm room-temperature, clear bore so that it could accommodate the main body of the autoclave; however, since, due to the length of the magnet and dewar, the autoclave had to be fully inserted into the 76 mm magnet bore, certain modifications had to be made to the water cooling system and the RF filters.

The autoclave (Figure 2) is a beryllium copper cylinder with a length of 420 mm. The largest outer diameter is 75 mm. The center portion of the outer surface of the autoclave has raised ridges that make contact with the inner diameter of an exterior brass cylinder to form a water jacket. The interior of the autoclave is machined so that pressure plugs may be inserted and secured with large

Autoclave

Not to scale

Material: Beryllium Copper

Side View - Cut Away

Side View - Exterior

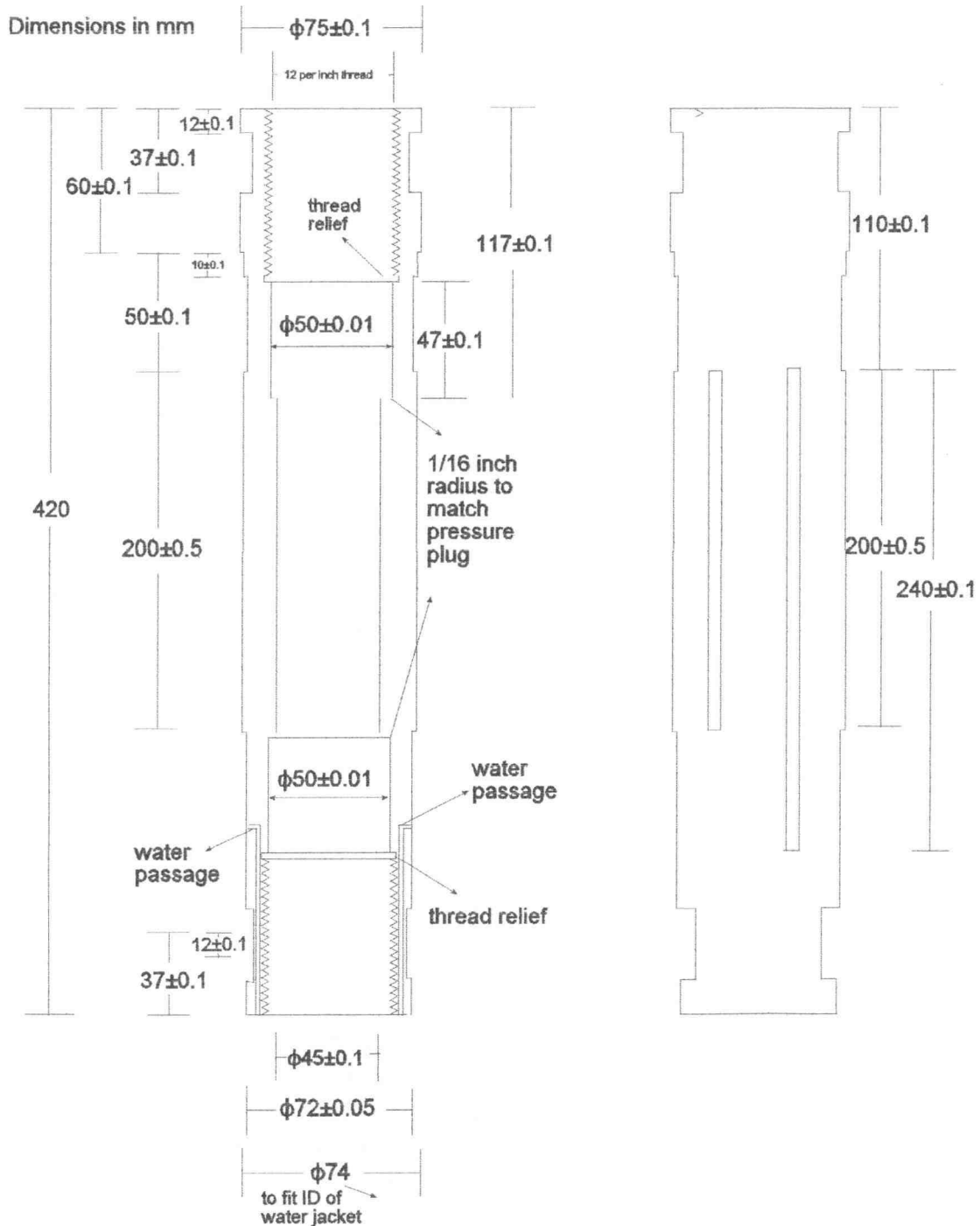


Figure 2 Pressure vessel (autoclave) to be used in spectrometer with 76 mm bore.

threaded screws. In the following sections are descriptions of modifications to the autoclave.

Water Cooling Channels

When the autoclave was constructed, water channels were machined before the beryllium copper was tempered. A seamless water jacket fit tightly against the ridges of the water channels. The bottom of the water jacket butted against a ledge that was left when the water channels were machined. The bottom of the water channel was closed using a ring that had been machined to fit tightly against the autoclave at the bottom edge of the ring and to fit under the water jacket at the top edge of the ring. The ring also provided a base for the Swagelock® fittings that allowed the entry and exit of cooling water. The water jacket and ring were sealed to the water jacket with an adhesive.

Due to the age of the adhesive, certain areas around the perimeter of the water jacket, ring, and autoclave seals had developed leaks. Unfortunately, the adhesive had not degenerated enough to allow the removal of the water jacket using nondestructive methods. The water jacket and ring had to be carefully cut away from the main body of the autoclave.

Since the water fittings that extended diametrically from the autoclave would render the assemblage too large to fit into the magnet, it was decided to introduce cooling water using a design that would be parallel to the axis of the autoclave. Several designs were considered, but the

final choice was a design that required the machining of additional water channels in the autoclave. The machining of the autoclave presented numerous difficulties. The autoclave is constructed from beryllium copper that was machined and then tempered; if the temperature of the tempered beryllium copper is raised above approximately 100 degrees Celsius then the metal begins to lose its temper and must be retempered. Repeated retempering, however, could destroy the integrity of the pressure vessel. Since the water channels were to be drilled into the bottom of the autoclave where the walls were 12.5 mm thick and where the autoclave was to be subjected to a relatively small amount of pressure, it was decided that if proper precautions, such as the liberal use of oil while machining, were taken that the channels could be machined without weakening the pressure vessel. Exhaustive pressure tests were performed on the autoclave after the machining was completed to insure the safety of the autoclave. It should also be noted that, when beryllium copper is machined, face masks should be used because beryllium copper dust is hazardous. The outer portions of the water channels were tapped to allow the connection of tubing. The water cooling channels are visible in Figure 2.

The water jacket was replaced with a brass cylinder that was turned on a lathe. Both the interior and exterior of the cylinder had to be worked with the lathe. A ring was machined that allowed the water to enter from the new water channels while preventing the loss of water from the water jacket. The ring and water jacket were fastened to the autoclave using adhesive.

The main seals of the pressure system are secured with large screws which thread into the ends of the autoclave. With the relocation of the water lines, the bottom screw became unusable since the water lines interfered with the head of the screw. It was necessary to machine the screw head into a smaller diameter. At this time, we took the opportunity to make the screw easier to tighten by machining the head of the screw into a hex-head shape instead of the previous cylinder shape with wrench flats.

O-ring Adapter

The intended use for the autoclave was liquid samples at increased pressure. Since liquids have a tendency to expand under pressure, it was necessary to have a reservoir into which the liquid could expand. Due to size constraints, this reservoir had to be placed outside of the autoclave. This placement necessitated a feedthrough that did not compromise the pressure integrity of the autoclave, but which allowed the fluid to expand. Since the reservoir tubing and the sample cell capillary tubing could not be permanently attached, it was necessary to design an adapter to allow the tubing to join. This adapter, illustrated in Figure 3, also functions as the anchor for the sample cell. When not using a liquid sample, the adapter can be used solely as the sample cell anchor by inserting a solid piece of rod into the upper portion of the adapter. Care must be taken, however, that the rod used to blank off the channel is non-magnetic in high magnetic fields.

O-ring Adapter

Material: non-magnetic stainless steel

Scale: 4:1

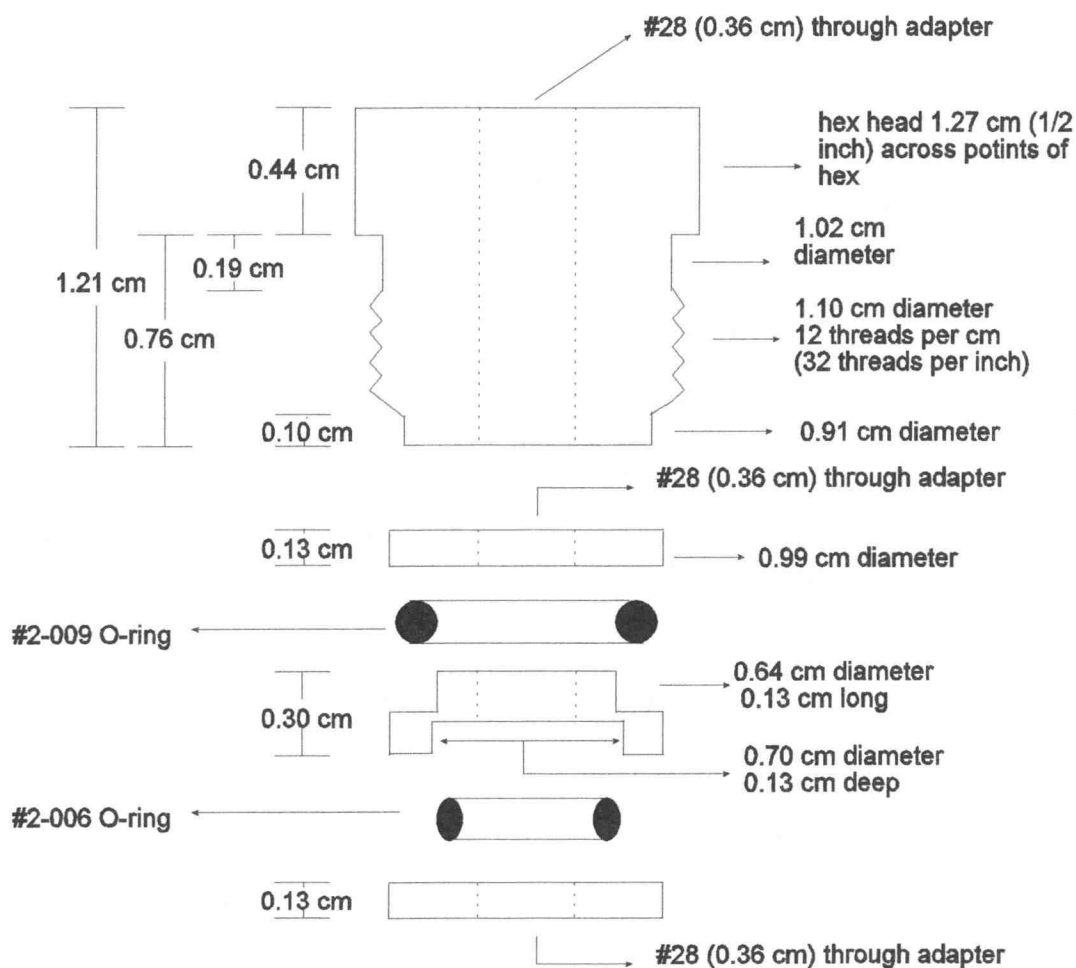


Figure 3 Adapter to allow connection of interior and exterior liquid sample tubing through top of autoclave without loss of pressure.

Sample Cell and NMR Coil

In NMR, the RF coil must lie perpendicular to the applied magnetic field. In the iron magnet, this requirement allowed the RF coil and sample cell to lie axially in the autoclave. However, since a superconducting magnet is solenoidal, the new version of the RF coil must lie diametrically in the autoclave. This severely limits the size of the sample cell and the RF coil.

The largest interior diameter of the autoclave is 50 mm. This space must accommodate a sample cell, RF coil and leads, a heater, and insulation. The heater that was used previously was sufficient for our purposes and did not need to be redesigned. The heater consists of three individually controllable heating elements. The elements are molybdenum wire non-inductively wound on alumina forms. The interior diameter of the heater is 15.9 mm.

Originally, we planned to use 0.8 mm diameter copper wire for the RF coil; this lead us to limit the size of the sample cell to a cell 8.0 mm in diameter and 9.4 mm in length. Two similar, but different, sample cells have been designed. The first cell is designed for use with reactive, liquid samples at high temperatures (Figures 4, 5, 6, 7). The second cell is designed for use with solid samples at low temperatures.

The first cell is constructed of alumina tubing with a machined alumina cap. A capillary tube connecting the cell to the top pressure plug provides physical support and allows for the expansion of liquid samples. The capillary tube has had indentations machined near the body of the

Sample Cell Assembly

Material: alumina

Scale: 4:1

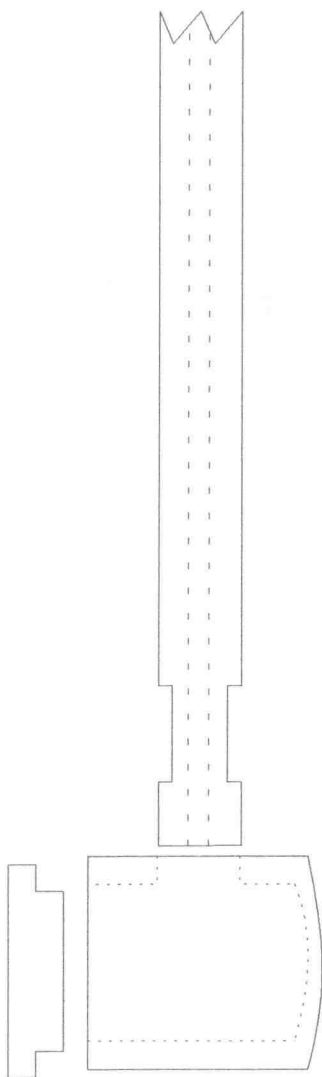


Figure 4 Sample cell for use with liquid sample (Assembly Drawing).

Delivery Tube

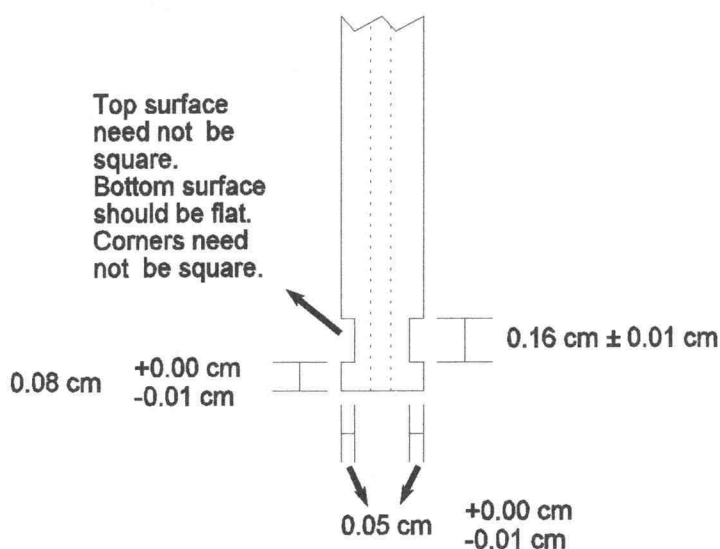
Material: 0.32 cm 2-bore 996 alumina tubing

Scale: 4:1

End View



Side View



Scale: 1:1

Side View - Length

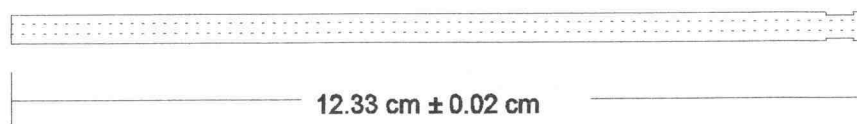


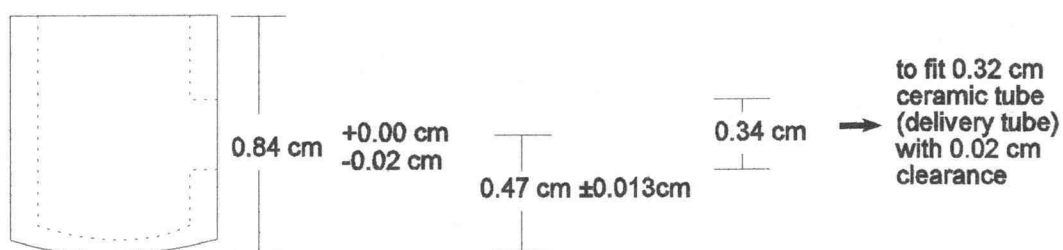
Figure 5 Manufacturing drawing of delivery tube to be used with liquid samples.

Sample Cell

Material: Single-bore alumina tubing

Scale: 4:1

Side View-1



Side View-2

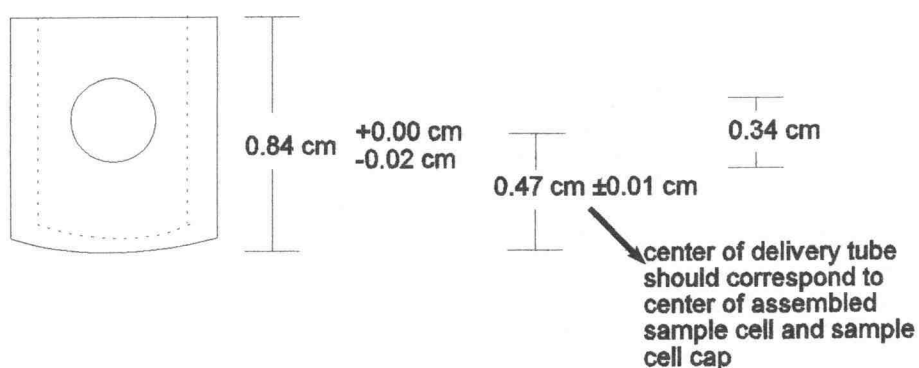


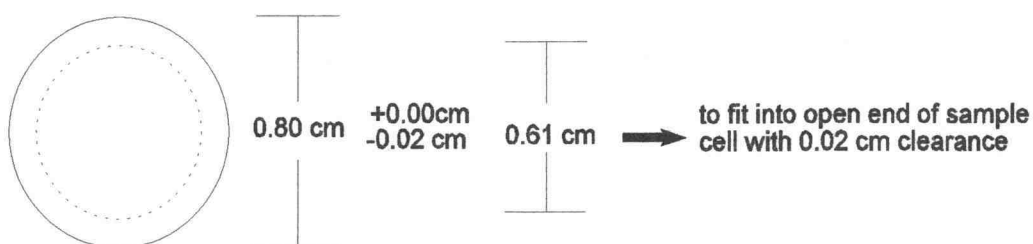
Figure 6 Sample cell for use with liquid samples.

Sample Cell Cap

Material: 1.27 cm 996 alumina rod

Scale: 4:1

Top View



Side View

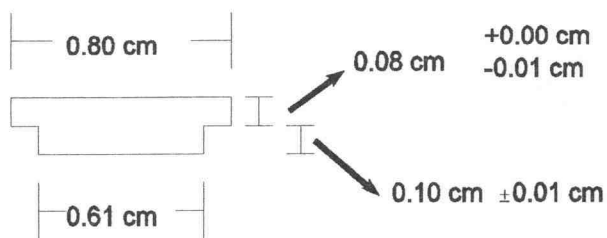


Figure 7 Cap for sample cell to be used with liquid samples.

cell; these indentations allow a more even winding of the RF coil. The cell, cap, and capillary tube are bonded together with powdered alumina. Care must be taken not to use adhesives or cements that contain zirconia since zirconia becomes conducting at high temperatures. If experiments are to be performed on liquid metals, it is desirable to use 0.5 mm OD alumina tubing in the body of the cell to increase the effective surface area of the sample.

The sample cell to be used for solid samples has the same basic design as the cell to be used for liquids with a few differences. If this cell is to be used at temperatures below 1000 degrees Celsius, the cell may be constructed from quartz, or if the temperatures are to be below 500 degrees Celsius, Pyrex may be used. The open end of the cell may be closed using a material such as alumina felt. The capillary tube used in the alumina cell is replaced with a solid rod which provides physical support.

In an effort to minimize the inductance of the coil leads, it was decided to use 2 mm wide strips of foil instead of 0.8 mm diameter wire in the winding of the RF coil. The autoclave was tested to a temperature of 448 K; this allowed the use of Cu foil for the RF coil. At the temperatures required to study phase transitions in liquid metals, a metal with a higher melting point, such as molybdenum, must be used to form the coil.

Since a crystalline sample with a low transition temperature was used to test the autoclave, a Pyrex sample cell closed with insulating felt was sufficient. Due to the space consumed by the fused joint between the Pyrex

sample cell and support rod, fewer turns are possible in this coil than would be possible using the ceramic cell as a coil form. The coil used in the autoclave tests contained two and a half turns of 2 mm wide strips of Cu foil. The coil was attached to the top pressure plug with 89 mm leads of 2 mm wide strips of Cu foil. The coil and leads were constructed of a continuous strip of Cu foil; this construction allowed for minor adjustments in lead length and turn spacing. At the pressure plug, the leads were connected via solder jacks to wires that went through the pressure plug via pressure feedthroughs. One coil lead and its attached wire were grounded to the pressure plug.

To minimize convection currents, the space below the sample cell was filled with alumina bubbles. Care must be taken that the bubbles do not press against the sample cell causing movement or breakage. In the area above the sample cell, insulation is also desirable. Two different considerations govern the configuration of this insulation. The first consideration is the integrity of the coil; the second consideration is that of convection currents. The insulation that was used in the pressure test consisted of pieces of insulating felt shaped to fit around the coil leads and to fill the space in to top of the autoclave. These pieces of felt had the advantage of filling the available space and reducing convection currents. However, the felt pieces had to be handled carefully to insure correct placement and did not help stabilize the RF coil leads.

For the temperature test, reduction of convection currents was sacrificed in order to lend support to the RF

coil leads and to insure non-contact between the turns of the coil. The insulation consisted of several short lengths of alumina tubing. The alumina tubing was threaded onto the coil leads. The tubing precluded the possibility of the coil contacting the autoclave, and the weight of the tubing helped the coil maintain a more uniform shape.

It was desirable for the sample to be placed at a position in the autoclave in which the temperature was uniform and controllable. To gather the spectra at elevated temperature, the three-stage heater described above was used. The center element in the heater was monitored and controlled; the upper and lower elements were monitored. To place the sample in the most uniform and controlled environment, the sample cell was located 127 ± 2 mm below the top pressure plug. This placement necessitated 125 mm long coil leads which were a major source of fixed capacitance. To tune the coil, a simple two-capacitor circuit was constructed (Figure 8). The circuit consisted of tuning capacitor connected in parallel with the RF coil, and a matching capacitor connected in series with the RF coil; the matching circuit allowed matching to the 50 ohm output of a CMX-360 spectrometer. Both of the capacitors were high voltage coaxial variable capacitors with ranges of 5 pF to 25 pF. The range of frequencies available with this tuning circuit was 57 to 70 MHz.

The capacitor portion of the circuit was mounted to a circular circuit board that would fit inside the bore of the magnet. In addition to the capacitors, a BNC connector was mounted on the circuit board to allow the easy

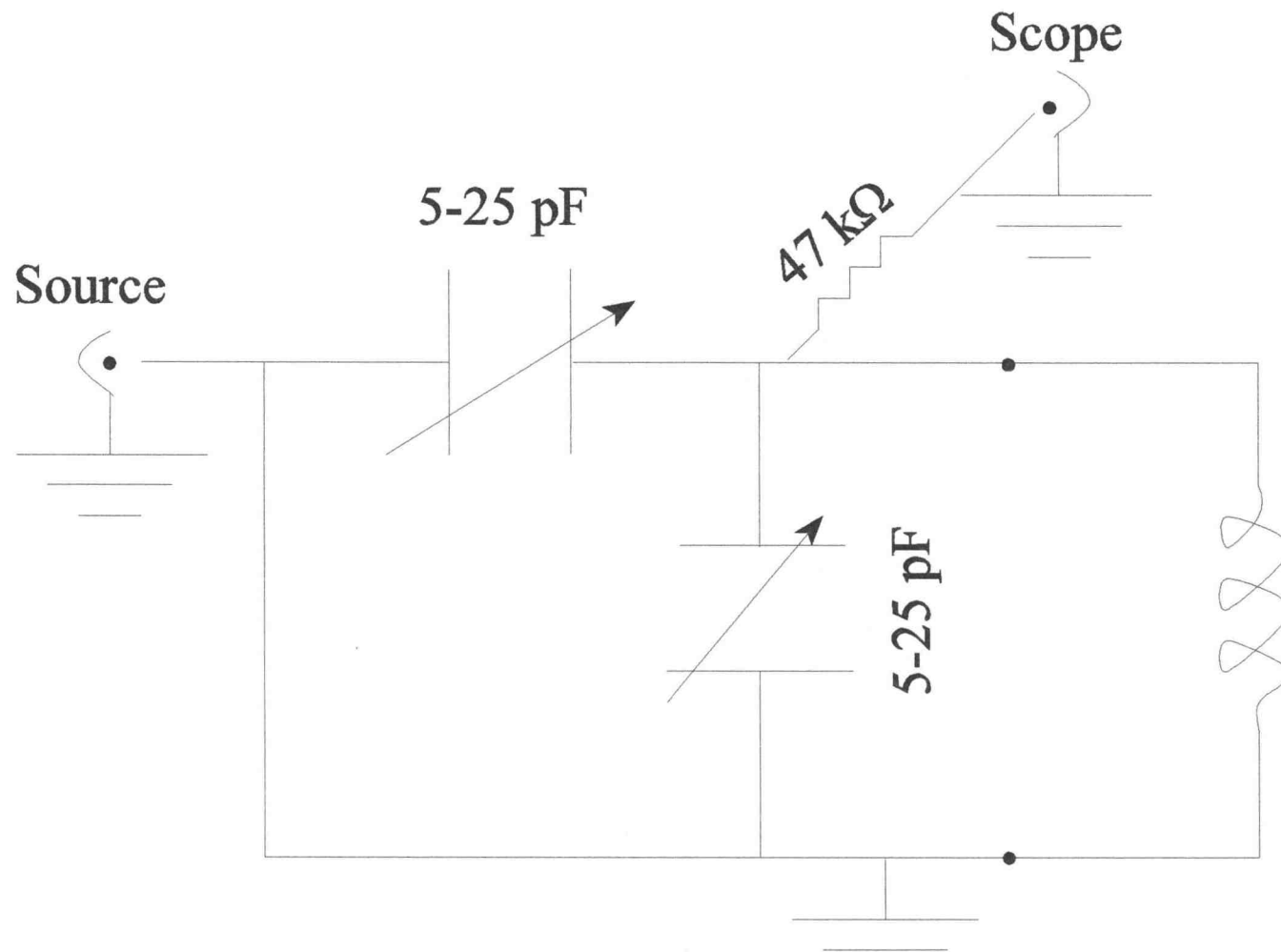


Figure 8 Tuning and matching circuit to allow resonant frequencies of 57 to 70 MHz.

connection to the RF pulse. The connections to the coil leads were made after the pressure seals on the autoclave were tightened to alleviate the possibility of weakening an electrical connection through stress. After the pressure plugs were tightened, the circuit board was mounted onto the top of the autoclave with two non-magnetic threaded rods and four non-magnetic nuts. The wires that were connected through the pressure plug to the coil leads were then soldered to the capacitor circuit.

Autoclave Support

To position the autoclave at the optimum position in the magnet dewar, a mount (Figure 9) was designed, which supported the autoclave and positioned it correctly. The support consisted of a cylindrical mount with machined channels to allow the passage of the water tubing; this mount was attached to a baseplate, which was then attached, with screws, to the bottom of the magnet dewar. The inner diameter of the cylindrical mount was sized to allow the hex head pressure screw on the bottom of the autoclave to set down into the top of the mount. The bottom edge of the autoclave then rested on the top of the mount. The mount then provided support as well as positioning. Component drawings are provided in Figures 10 to 13.

RF Filters

A second feature of the autoclave that was too large to fit into the magnet bore was the assemblage of RF filters for the heater and thermocouple leads. The filters

Autoclave Support Assembly Drawing

Material: Aluminum
Not to Scale

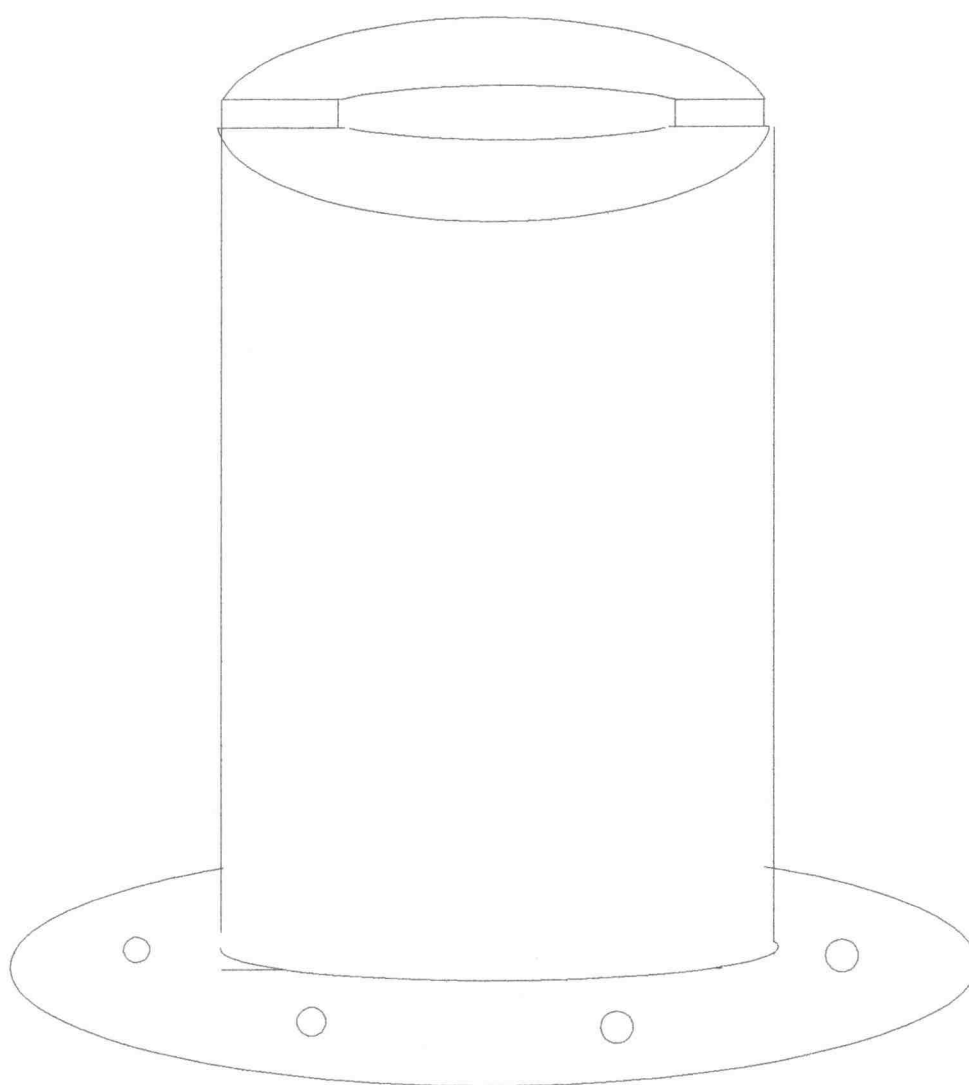


Figure 9 Mount to hold autoclave in the correct position with respect to the spectrometer.

Autoclave Support

Material: Aluminum

Scale: 3:4

Top View

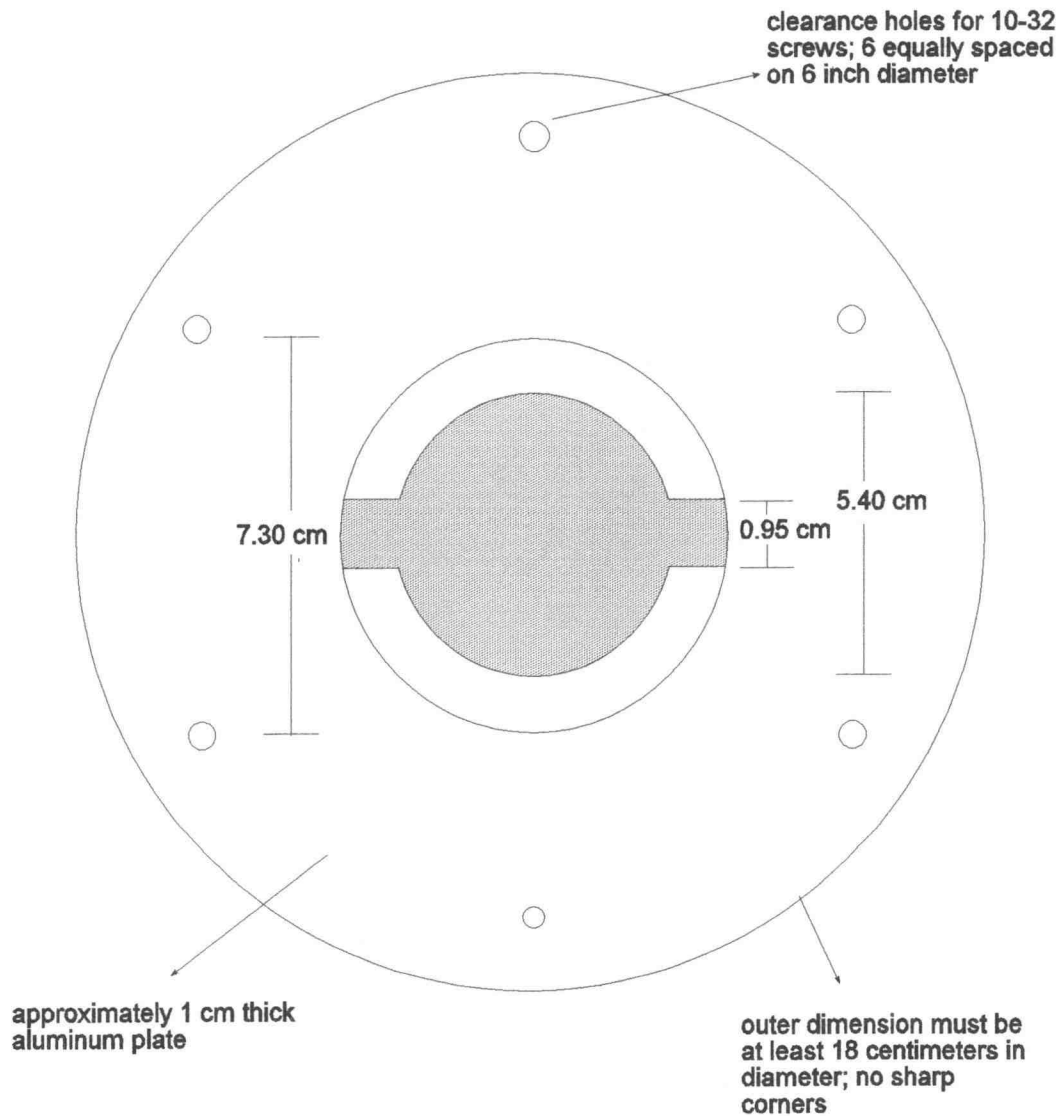


Figure 10 Top view of autoclave support.

Autoclave Support

Material: Aluminum

Scale: 3:4

Bottom View

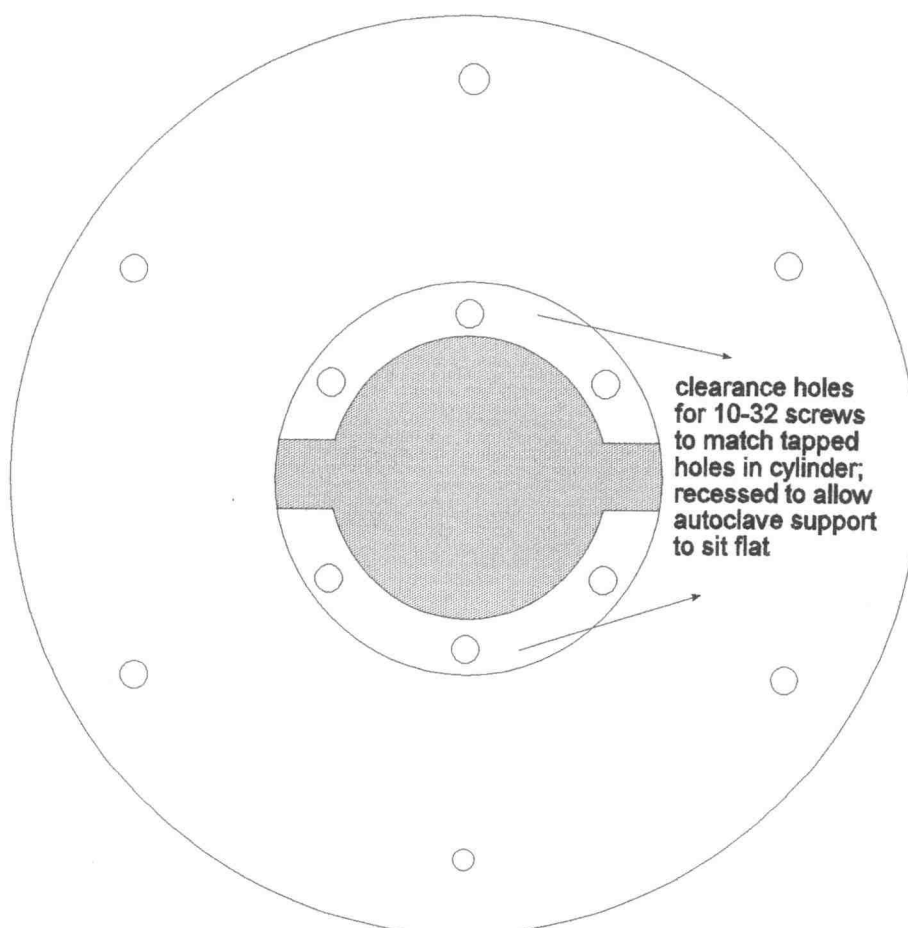


Figure 11 Bottom view of autoclave support.

Autoclave Mount

Material: Aluminum

Scale: 3:4

Bottom View

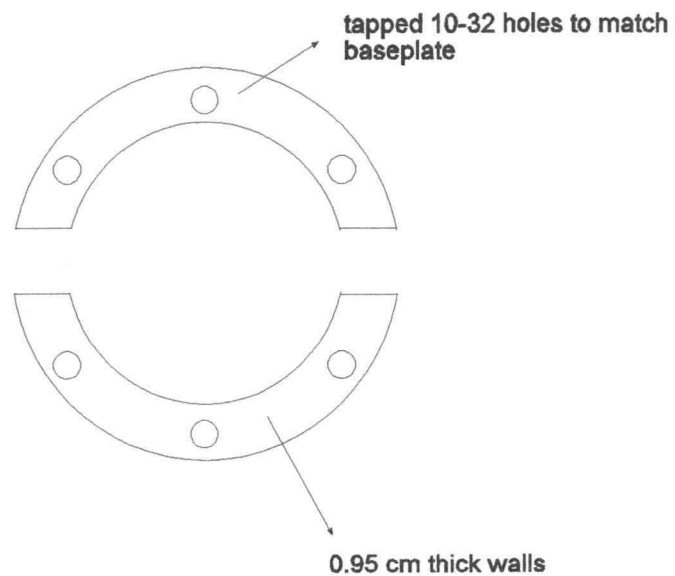


Figure 12 Bottom view of autoclave mount.

Autoclave Mount

Material: Aluminum

Scale: 1:1

Side View of Cylinder

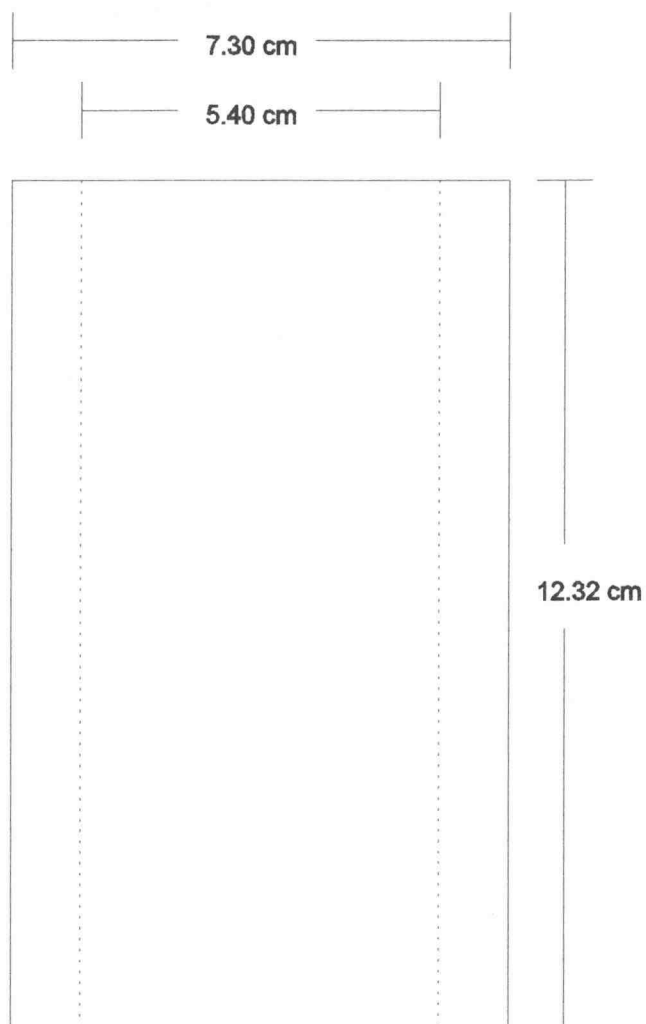


Figure 13 Side view of autoclave mount.

consisted of several inductors wound on ferrite cores; the inductors were contained in a metal cylinder that was attached to the bottom of the autoclave. Two problems were encountered with these filters. In addition to the size limitations, the ferrite cores had a tendency to saturate due to the strength of the magnetic field in the superconducting magnet. Several new filtering options were explored, but it was decided to modify the existing filtering system. It was discovered that the ferrite cores would saturate if closer than 180 mm to the lower edge of the magnet bore. Since the magnet dewar is 610 mm above the floor of the laboratory, it was possible to use the filtering system if the system was set on the floor. A physical support, reminiscent of the Lunar Lander (Figure 14), was developed for the filters.

Since the filters were no longer attached to the bottom of the autoclave, it was necessary to lengthen the heater and thermocouple leads. Initially, color-coded copper wires were soldered onto the heater and thermocouple leads. While this attachment method worked, the connections were fragile and cumbersome. A second method involved soldering male and female pin connectors to the leads and extension wires. These connectors made the connections less fragile and allowed the non-permanent connection of the wires. After the pins were connected, the connections were wrapped in Teflon[®] tape to prevent electrical contact between different thermocouples. Teflon[®] tape was used instead of regular electrical tape because the Teflon[®] tape did not have adhesive on it and could be easily removed when necessary.

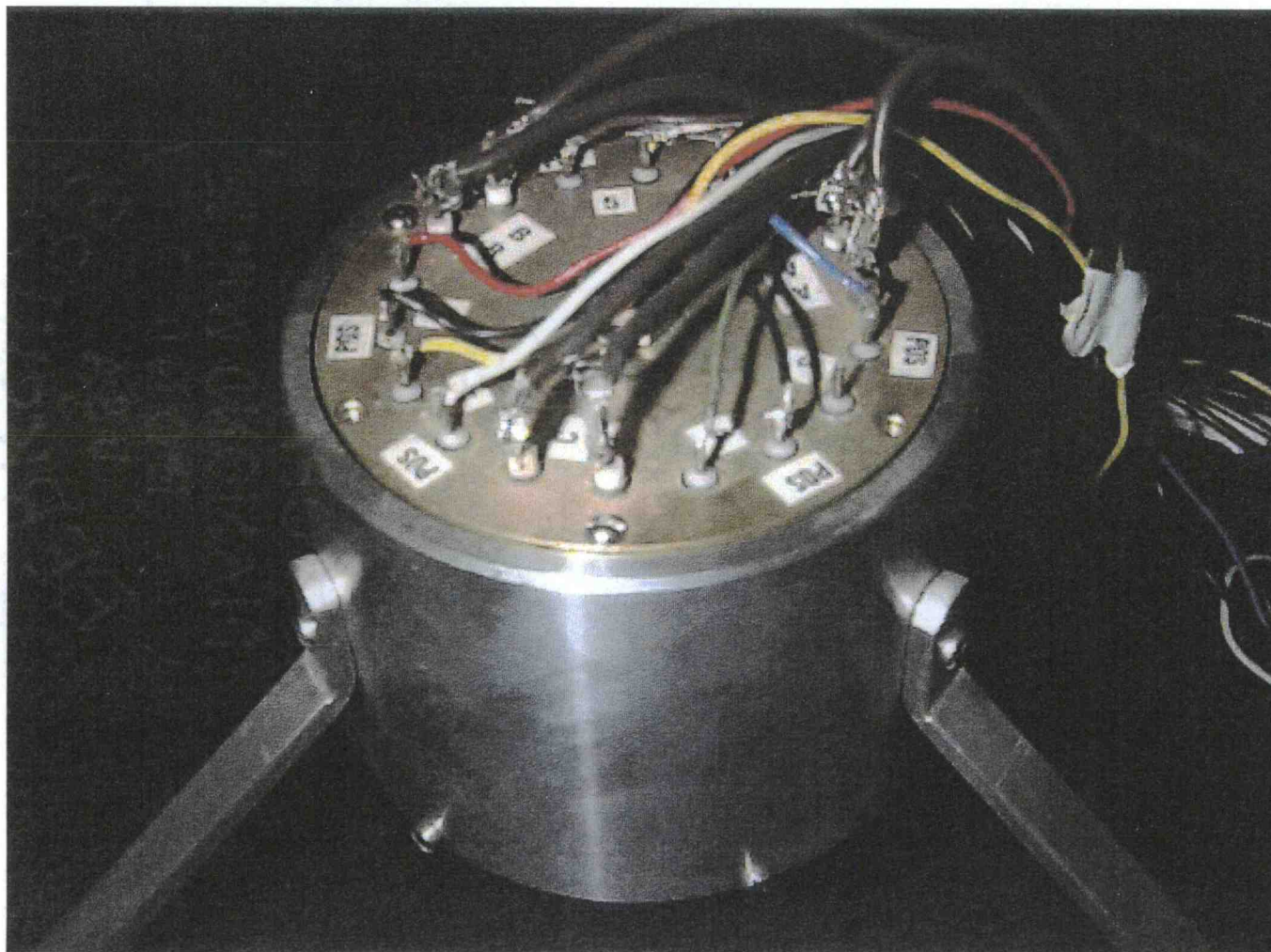


Figure 14 RF Filters (Lunar Lander)

EXPERIMENTAL PROCEDURE (CONSTRUCTION VERIFICATION)

To verify that the autoclave would perform as it was designed, spectra were observed using three different types of samples. The first sample, powdered GaAs, was chosen for availability and ease of use. The second sample, liquid Hg, was chosen to verify that the autoclave would be able to be used in future work with expanded liquid Hg. The third sample, AgI crystals, was chosen due to the presence of separate transitions at elevated temperature and at elevated pressure. All of these verifications were successful; however, each trial presented areas in which improvement could be made.

The first attempt to use the autoclave in the high field spectrometer used a bulk powder GaAs sample in a Pyrex[®] sample cell. Spectra were observed for room temperature and atmospheric pressure. This preliminary trial was successful, but no spectra were saved.

The next sample that was placed in the autoclave was a bulk liquid Hg sample in an alumina sample cell. Spectra were visible; however, due to the nature of the sample, the spectra were extremely noisy. This noise led us to develop methods for increasing the effective sample size. By increasing the surface area of the Hg sample, the effective sample size would be increased. The chosen method to increase the surface area consisted of filling the sample cell with small diameter, approximately 1 mm, alumina rod. An alternate method that was explored was the filling of the sample cell with small diameter alumina beads. The rods were chosen because the rods could be cut to a

specific length, thus ensuring that the sample cell cap would fit correctly. The Hg spectra displayed in Figures 15 to 17 were taken at room temperature and atmospheric pressure with no alumina rods in the sample cell.

To fully test the autoclave, two separate series of spectra were gathered using crystalline samples of AgI in Pyrex® sample cells. For the first set of spectra, the temperature was kept constant at room temperature and the pressure was varied between 1 bar and 1220 bar. Unfortunately, the spectra obtained at 1160 bar, 1200 bar, 1220 bar, and 1 bar after pressurization were either not recorded by the spectrometer or were lost during data transfer.

The first sample consisted of several small pieces of AgI. As seen in Figure 18, which was obtained at RTP before pressurizing the sample, the sample exhibits a powder pattern with strong quadrupole signals at -18 kHz and 16 kHz. The quadrupole interaction strength can be describe in terms of the resonant frequency and the central linesplitting in the following manner (Carter, 1977)

$$\left(\frac{e^2qQ}{h}\right)^2 = \nu_0 \Delta\nu \frac{64}{25} \frac{4I^2(2I-1)}{2I+3}.$$

Using the RTP $\Delta\nu$ of 34 kHz, the calculated quadrupole interaction strength, (e^2qQ/h) , is 8.6 MHz. This calculated quadrupole interaction strength is comparable, but larger, to that found by Segel et al (1969). As the pressure increases up to 1000 bar, the sample still exhibits the powder pattern and $\Delta\nu$ stays approximately constant (Figures 19, 20, 21, 22, 23). However, as the

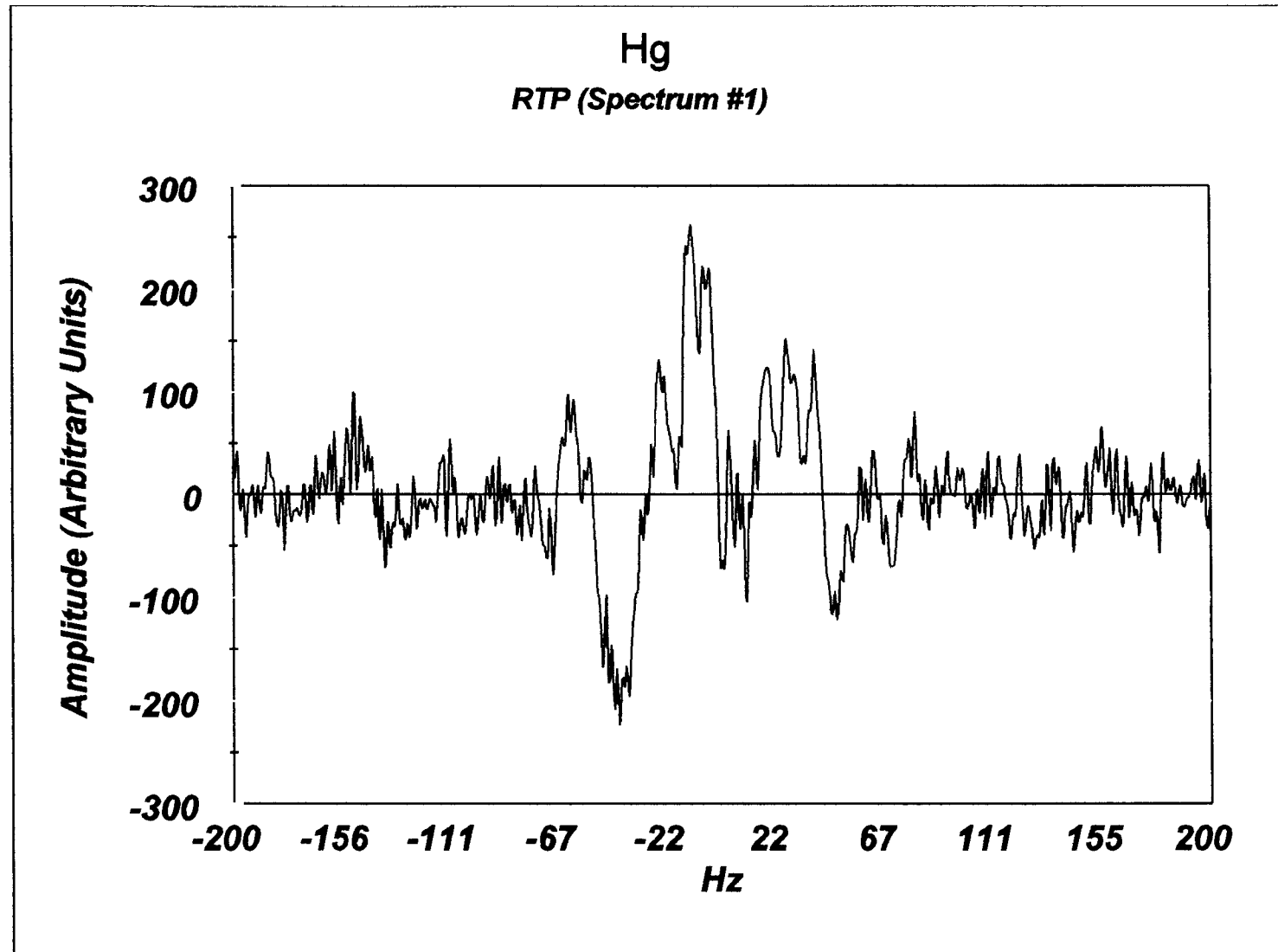


Figure 15 Liquid Hg spectrum gathered at RTP (Hg Spectrum #1).

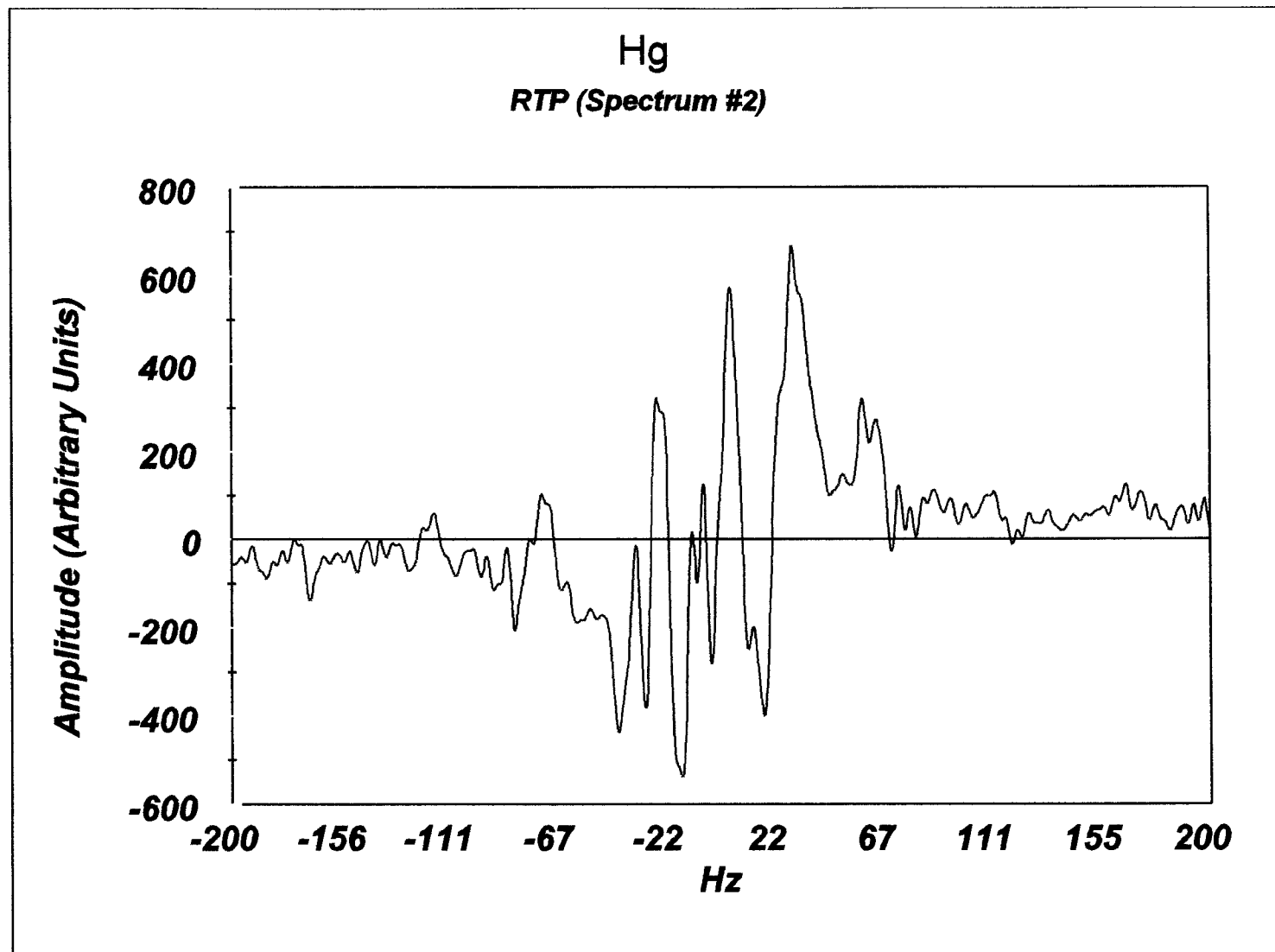


Figure 16 Liquid Hg spectrum gathered at RTP (Hg Spectrum #2).

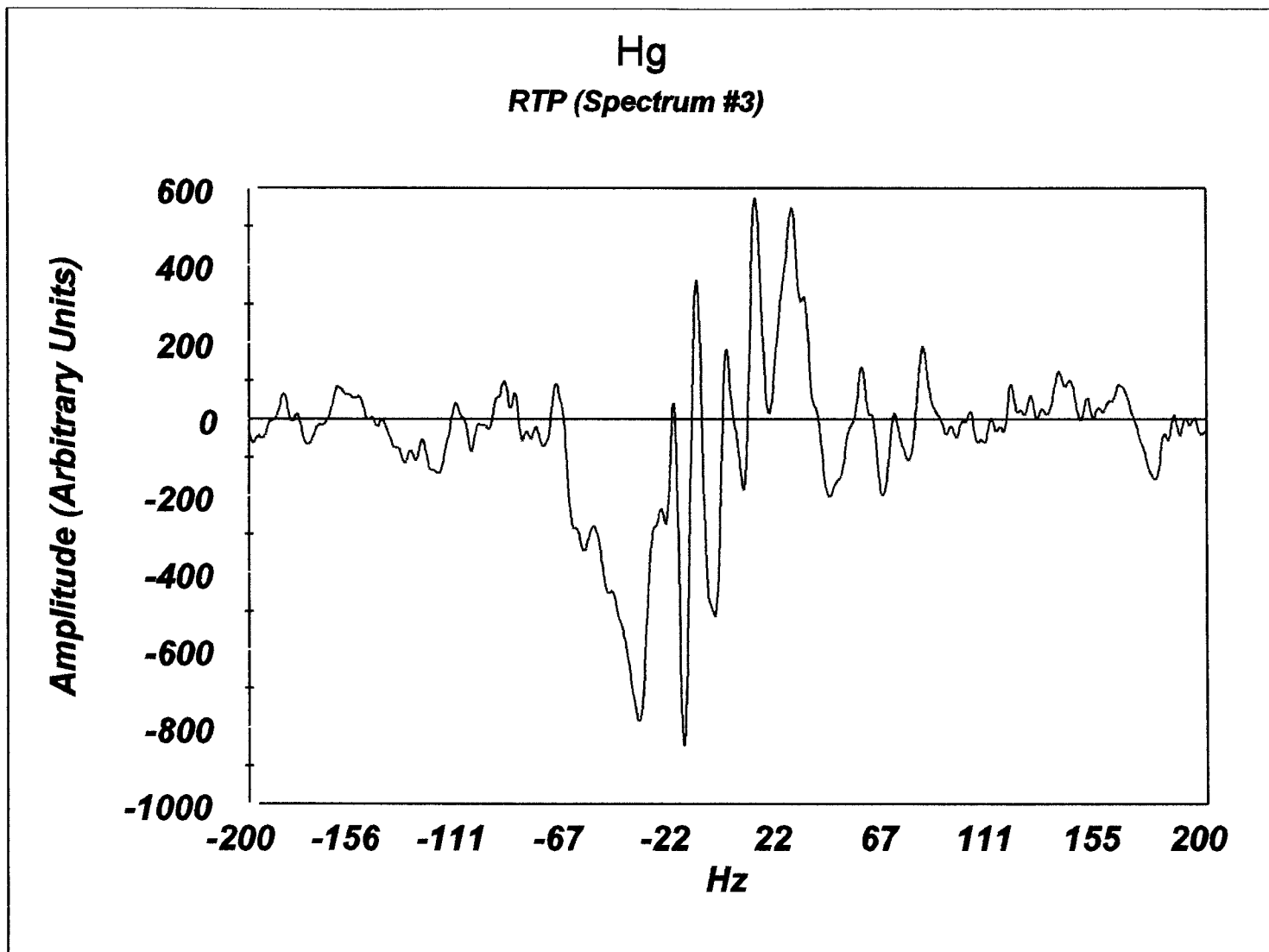


Figure 17 Liquid Hg spectrum gathered at RTP (Hg Spectrum #3).

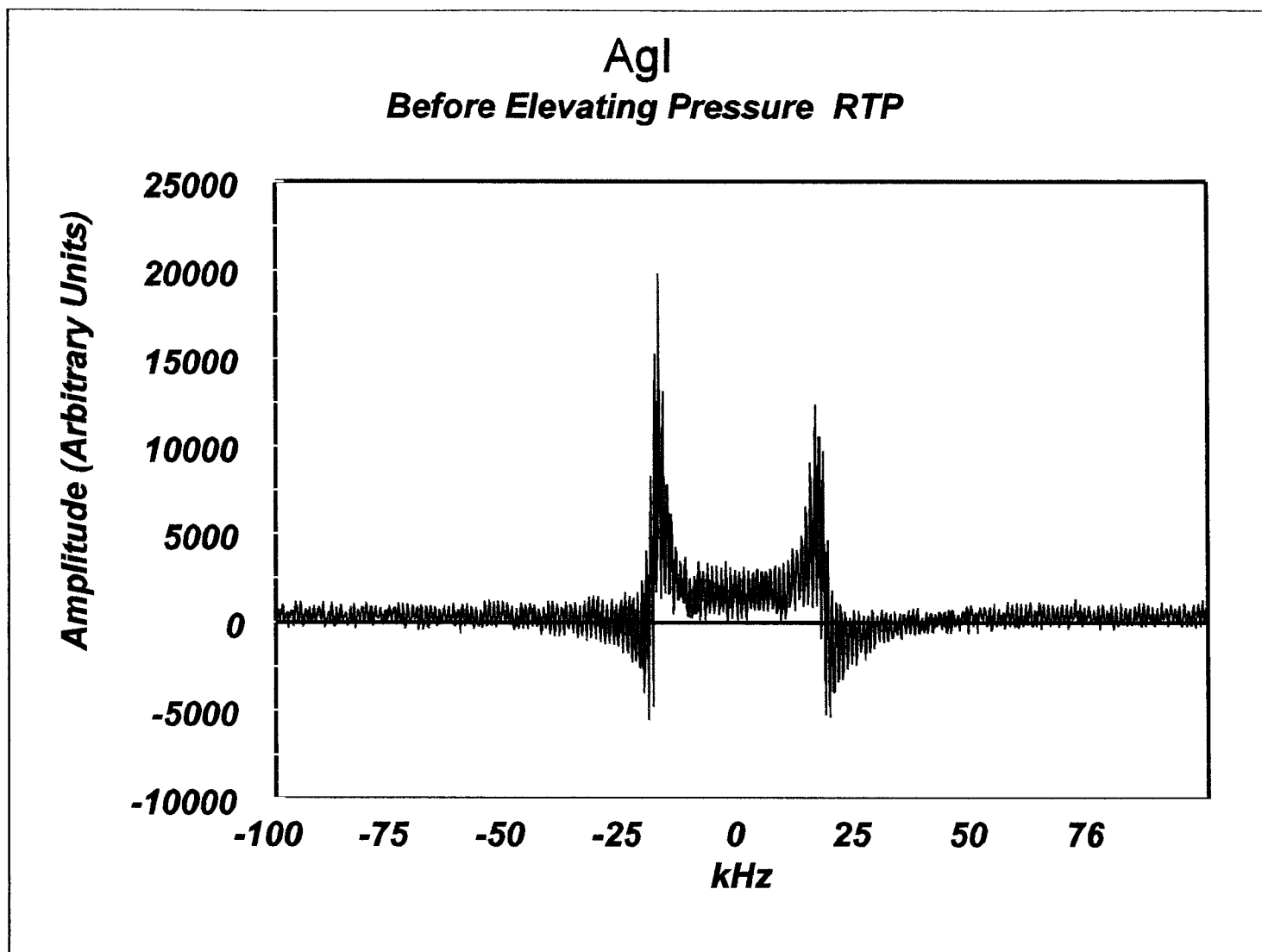


Figure 18 AgI powder at RTP before elevating pressure.

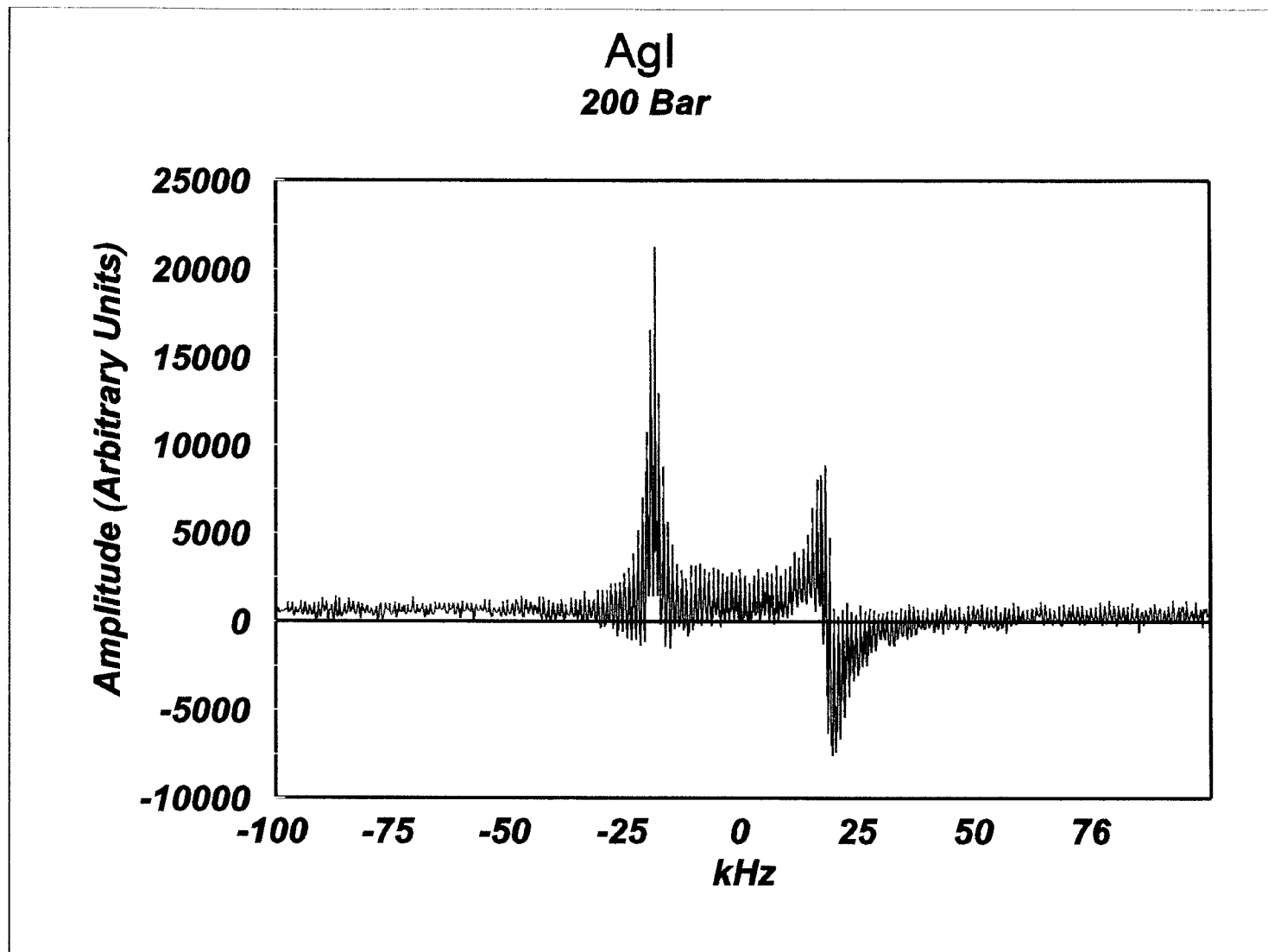


Figure 19 AgI powder at 200 Bar

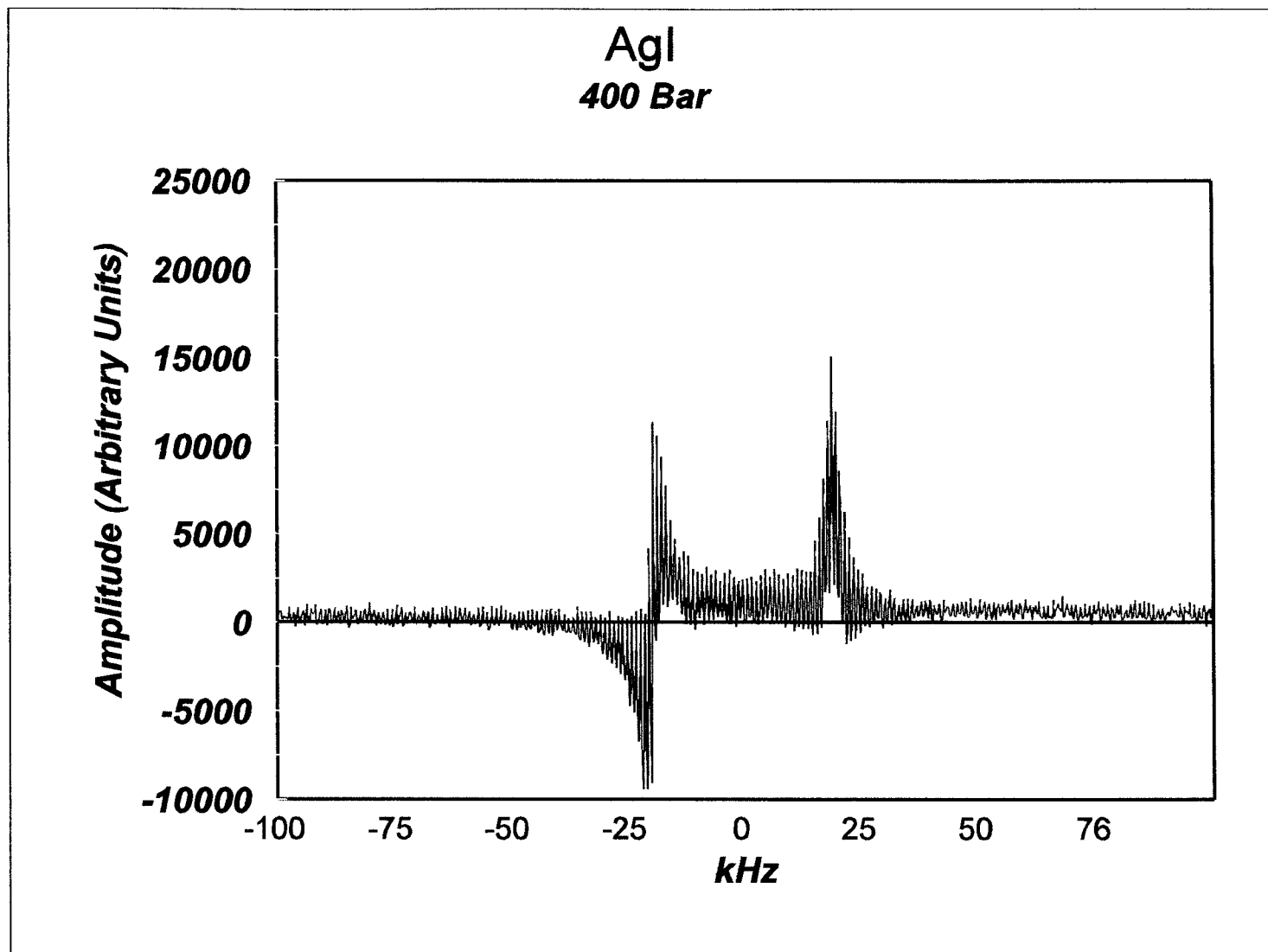


Figure 20 AgI powder at 400 Bar.

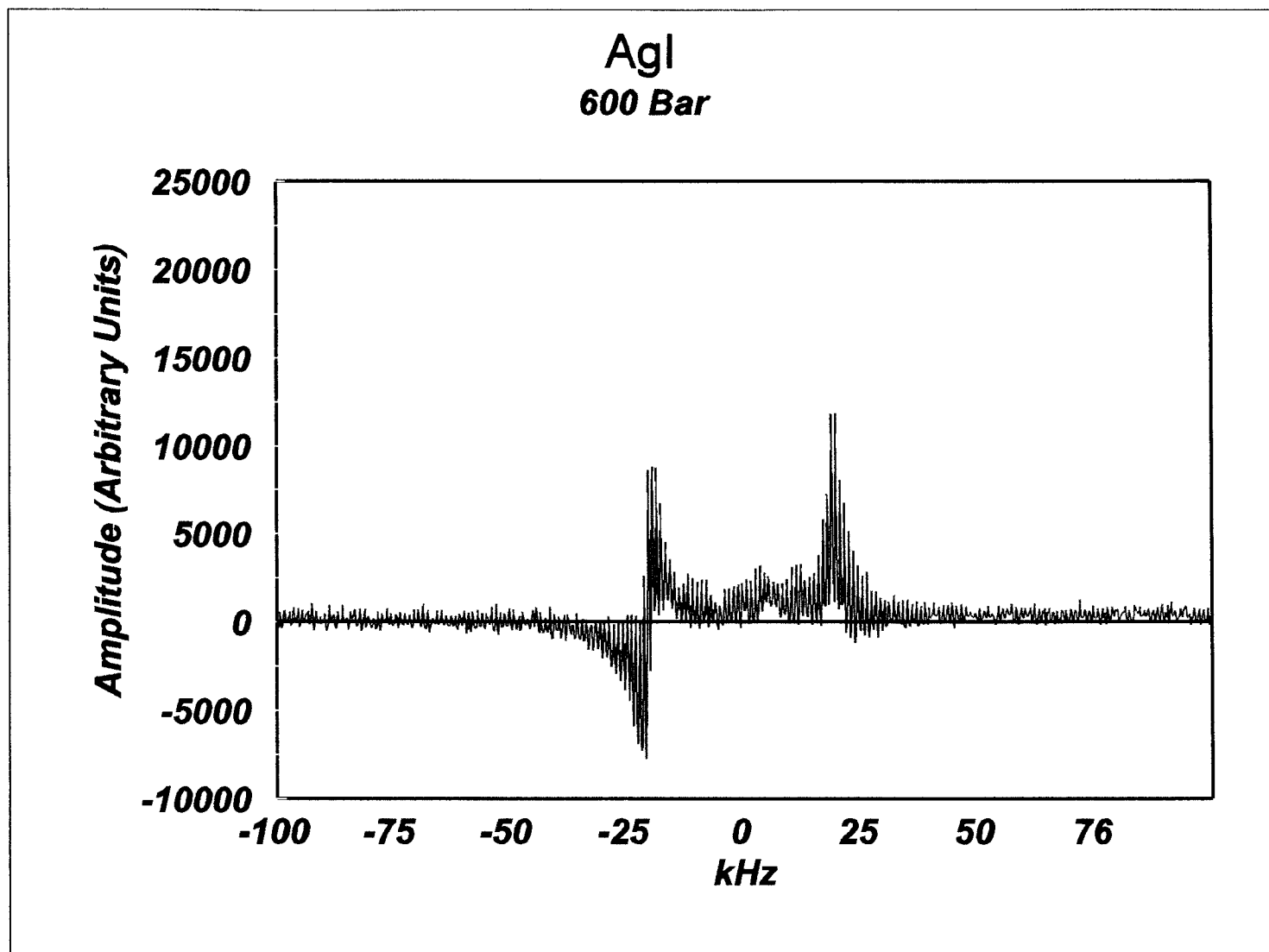


Figure 21 AgI powder at 600 Bar.

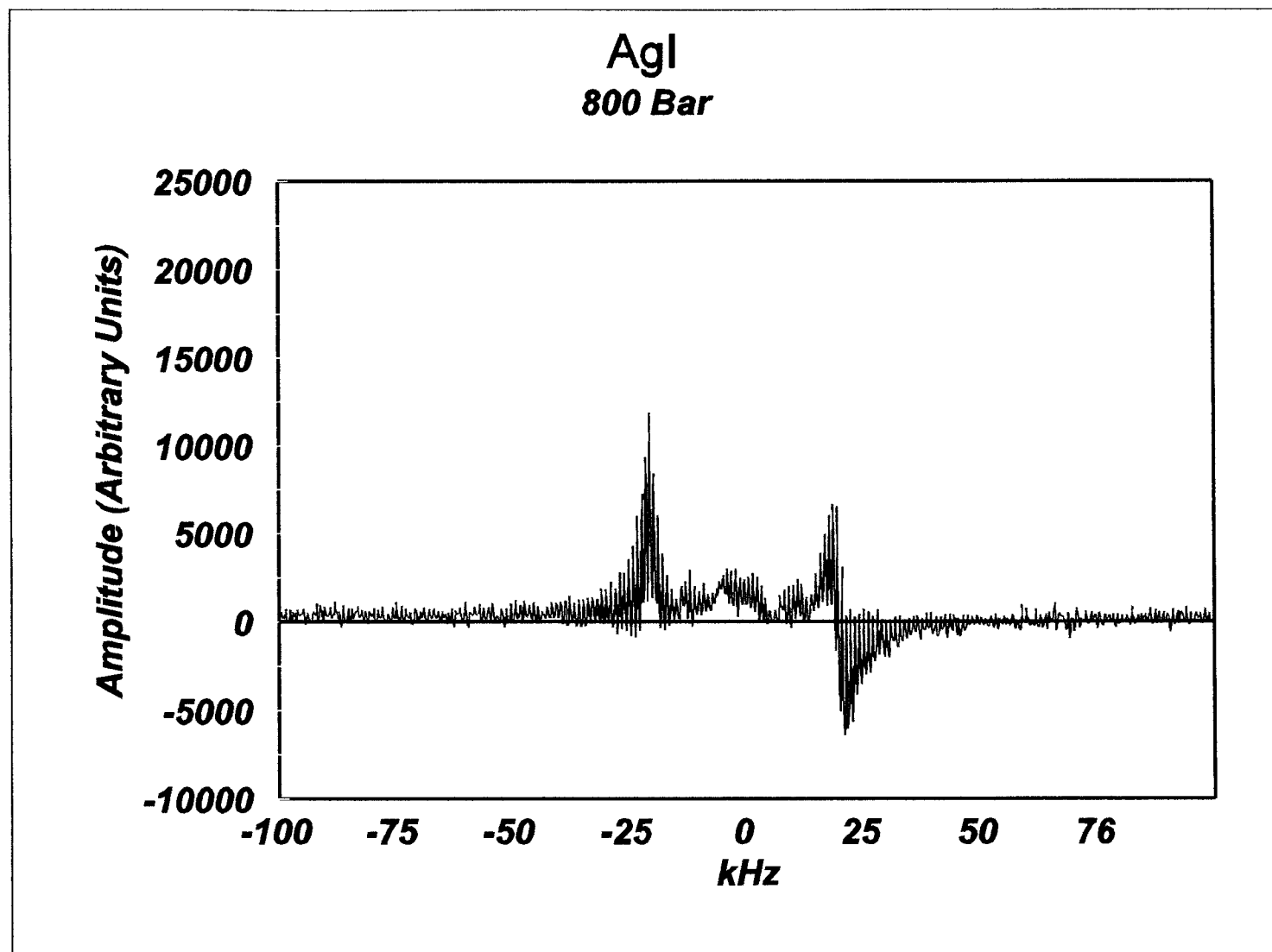


Figure 22 AgI powder at 800 Bar.

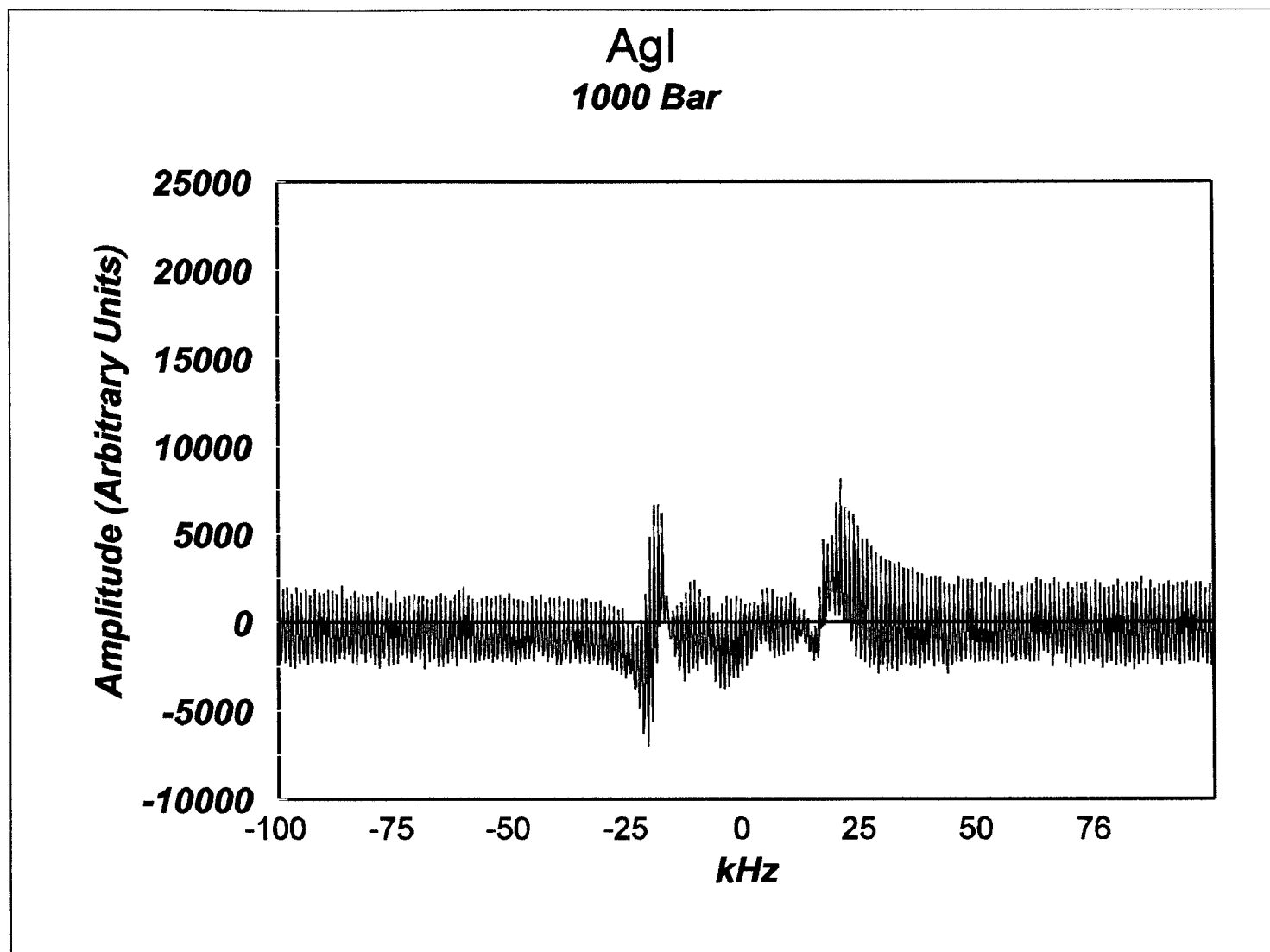


Figure 23 AgI powder at 1000 Bar.

pressure increases to 1100 bar (Figure 24), the quadrupole peaks move to -6 kHz and 3 kHz. With a $\Delta\nu$ of 9, the sample now has an (e^2qQ/h) of 4.4 MHz. This decrease in the quadrupole interaction may signal a structural transition. Studies by other researchers, using methods which include electrical conductivity, elastic constant measurements, and Raman spectra investigations, have also indicated the possibility of a transition near 1.1 kbar (Mellander, Bowling, and Baranowski, 1980). Others, however, have not seen evidence of this transition (Hoshino and Shimoji, 1972): This may be due to the time required to complete the transition (Mellander, Bowling, and Baranowski, 1980).

For the second set of spectra gathered from the AgI sample, the argon pressure was kept constant at atmospheric pressure and the temperature was varied between 295 K and 448 K. The sample for this set of spectra was a solitary crystal of AgI. The spectra displayed in Figure 25 through Figure 29 were gathered at temperatures below the transition temperature from the mixed β/γ phase to the α phase. In each of these spectra, a set of peaks is somewhat centered around the resonant frequency. The maxima of these peaks are at -13 kHz and 15 kHz. As the temperature is increased to 431 K, which is above the theoretical transition temperature, the peaks are still apparent, but have a slightly reduced amplitude. Figure 30 shows the spectrum gathered at 431 K. Since the temperature being monitored was that of the environment not that of the sample, this indication of the β/γ phase may be caused by temperature variation in the sample. The entire sample may not have reached the transition temperature at

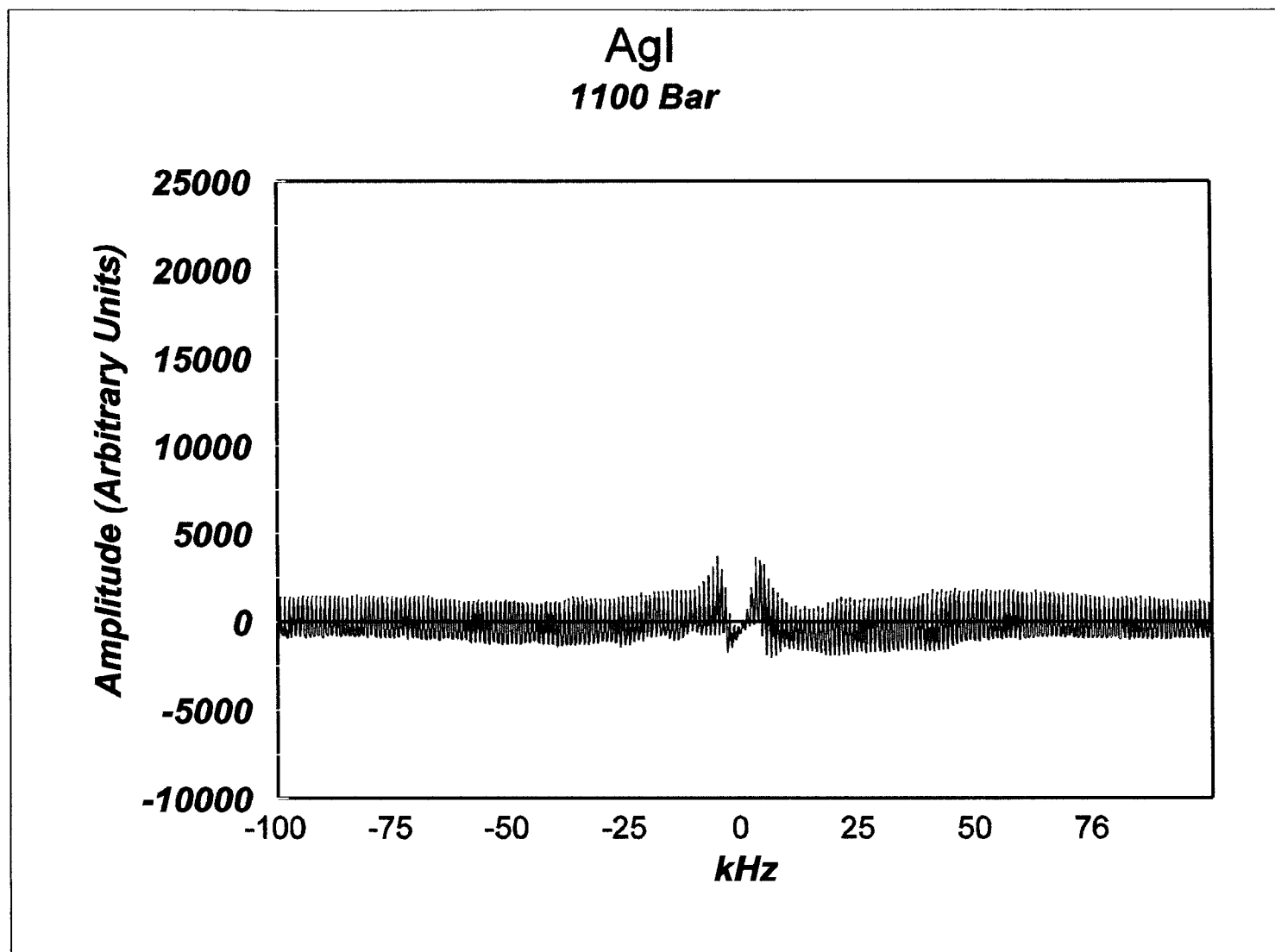


Figure 24 AgI powder at 1100 Bar.

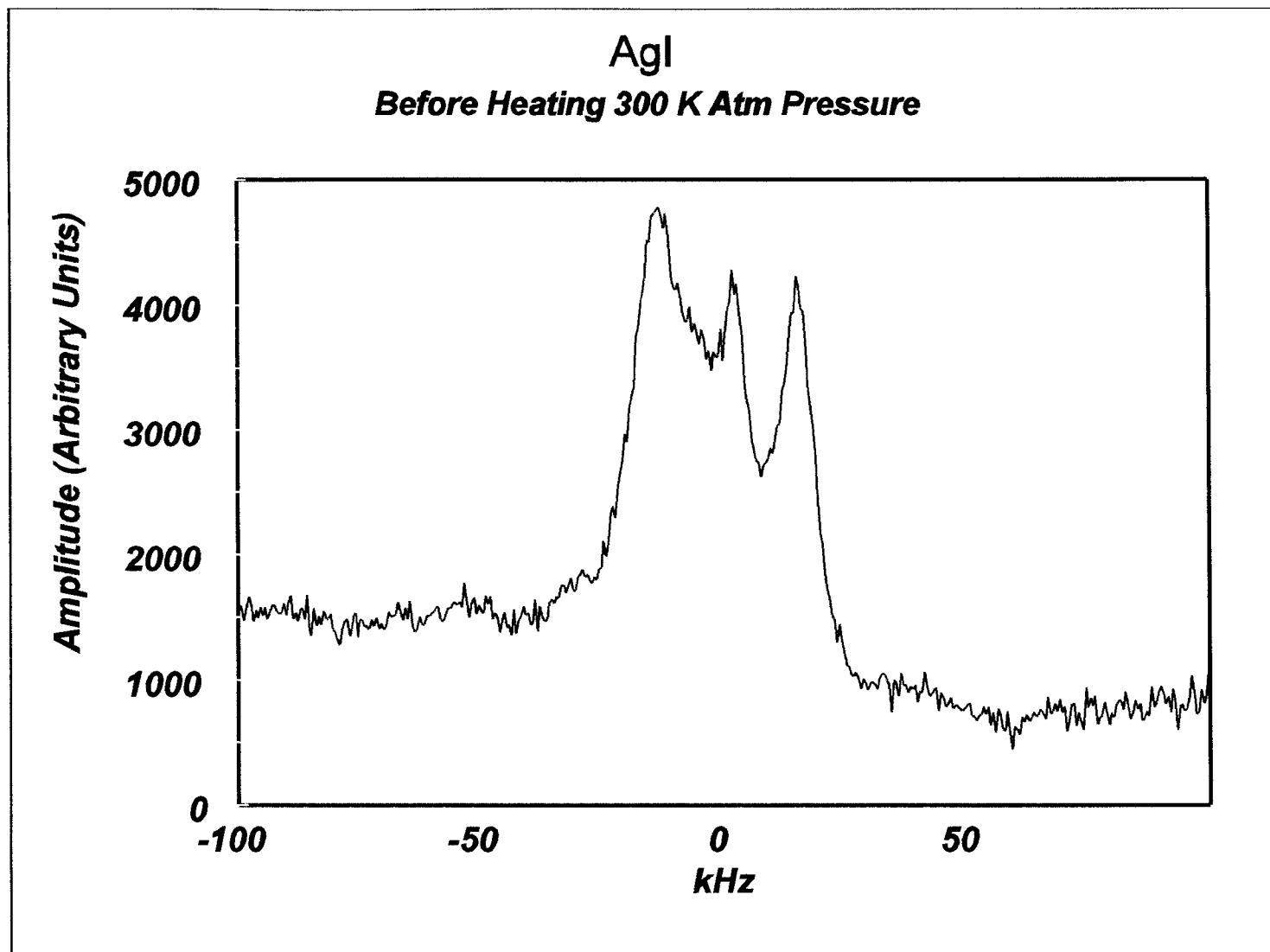


Figure 25 AgI crystal at RTP before heating

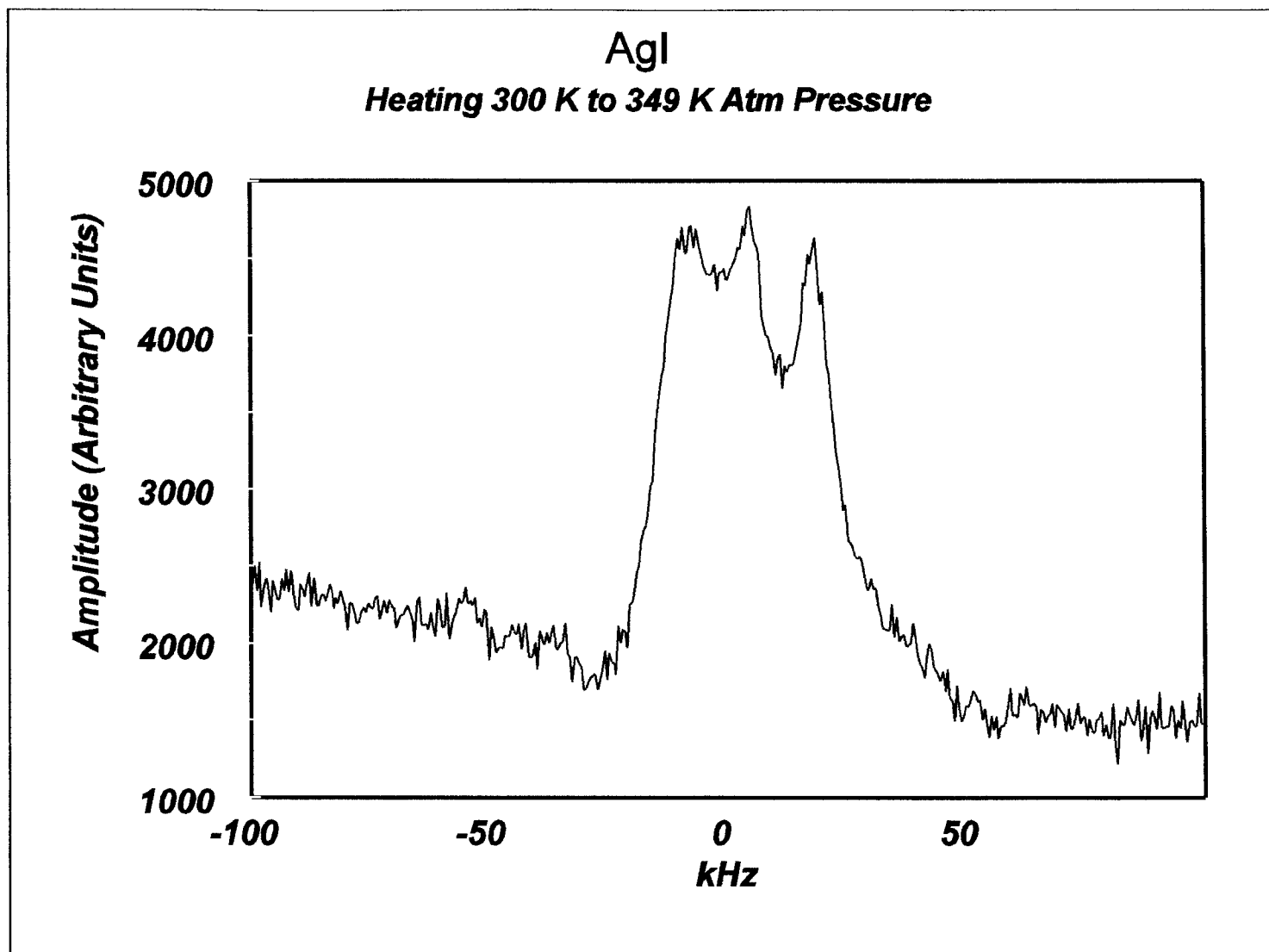


Figure 26 AgI crystal at atmospheric pressure during heating from room temperature to 349 K.

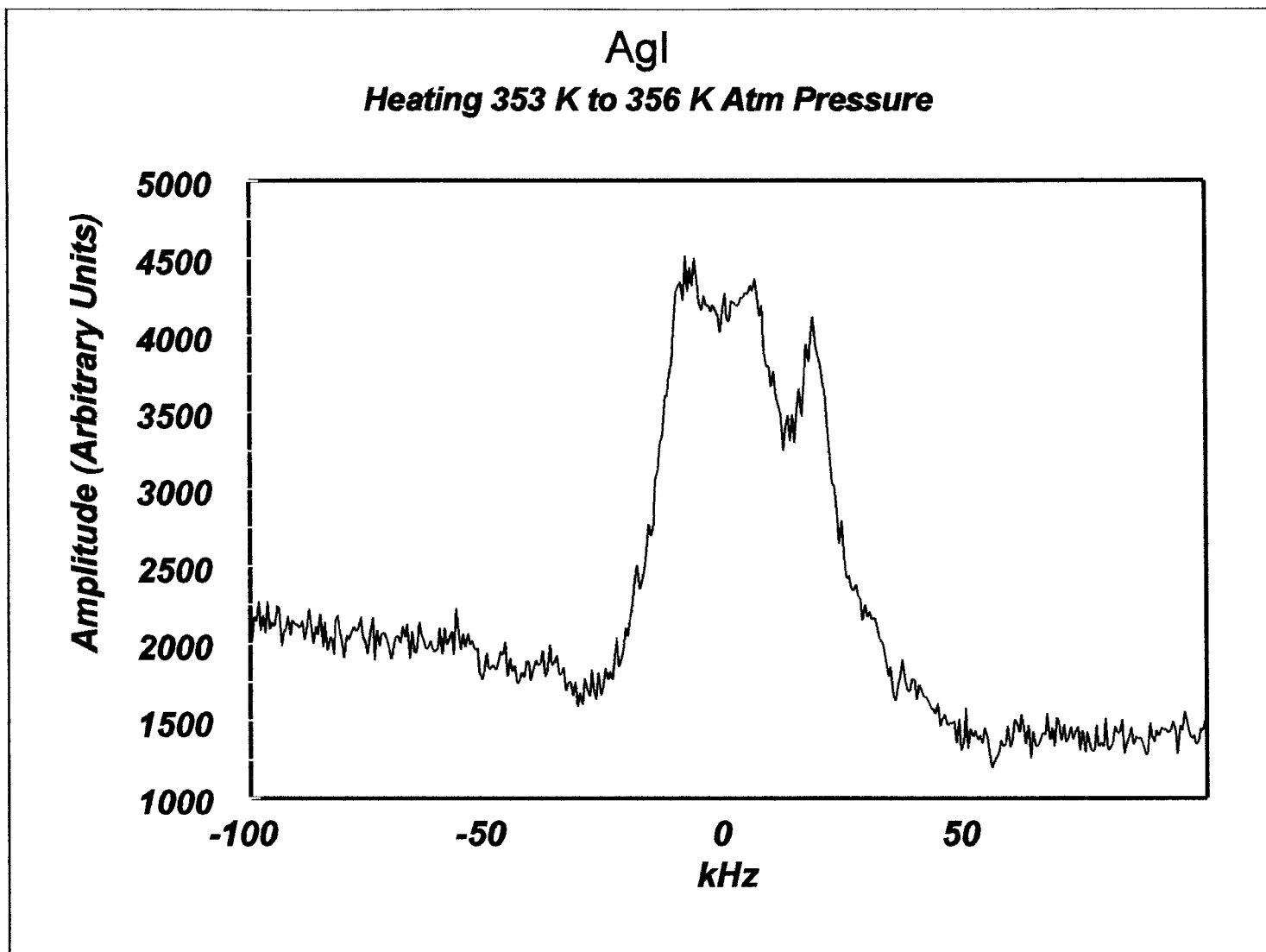


Figure 27 AgI crystal at atmospheric pressure heating from 353 K to 356 K.

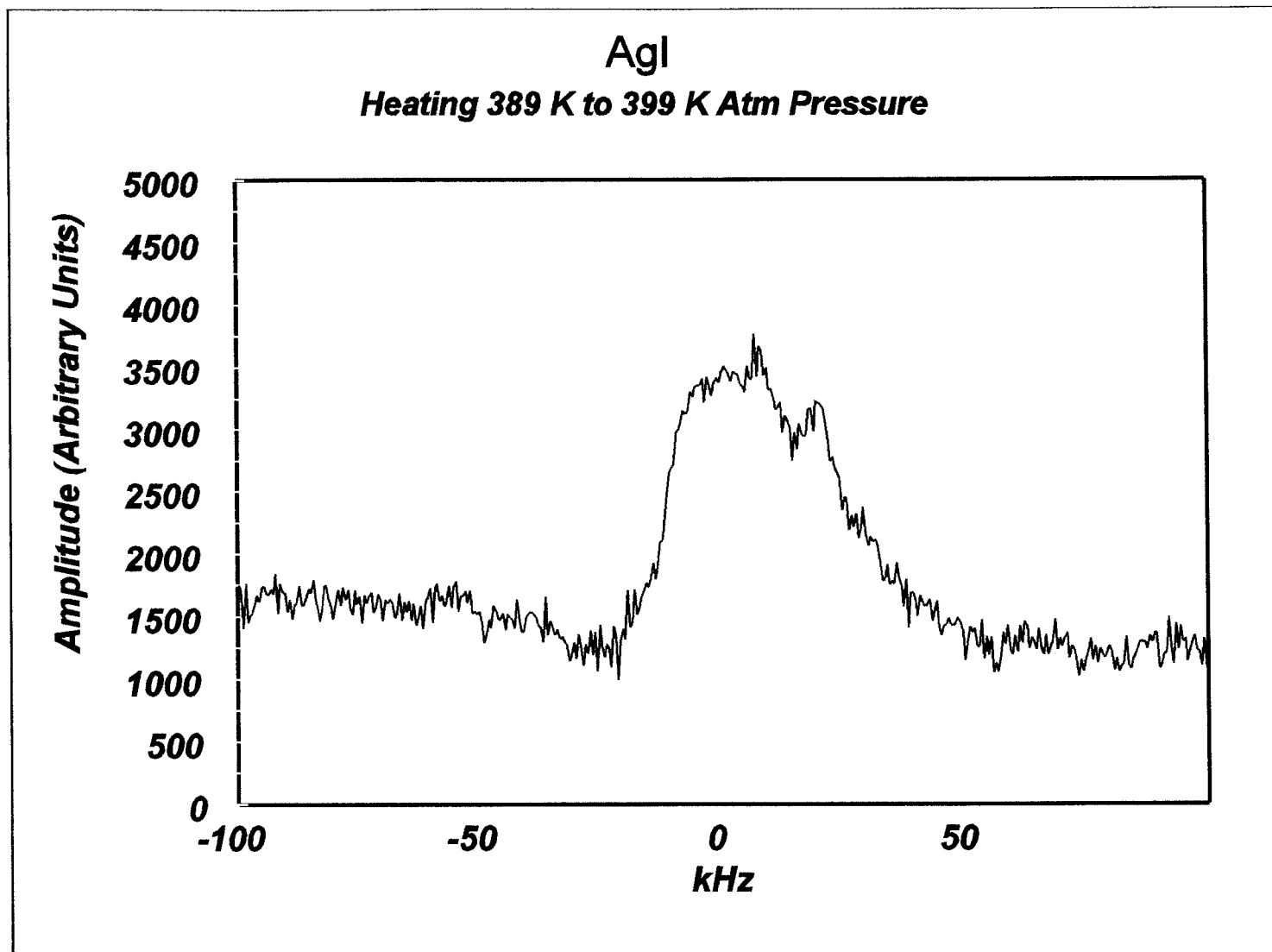


Figure 28 AgI crystal at atmospheric pressure during heating from 389 K to 399 K.

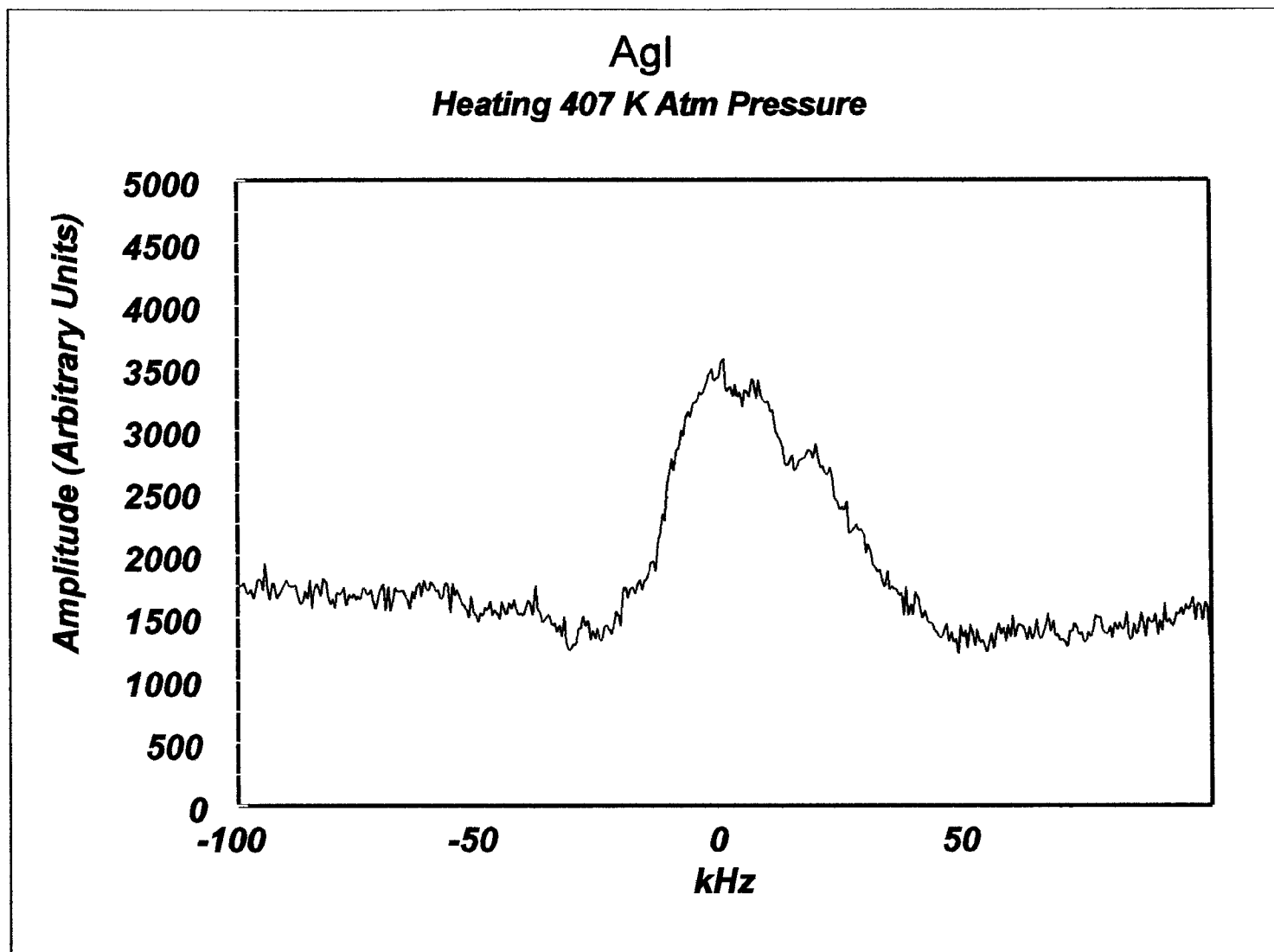


Figure 29 AgI crystal at atmospheric pressure and 407 K.

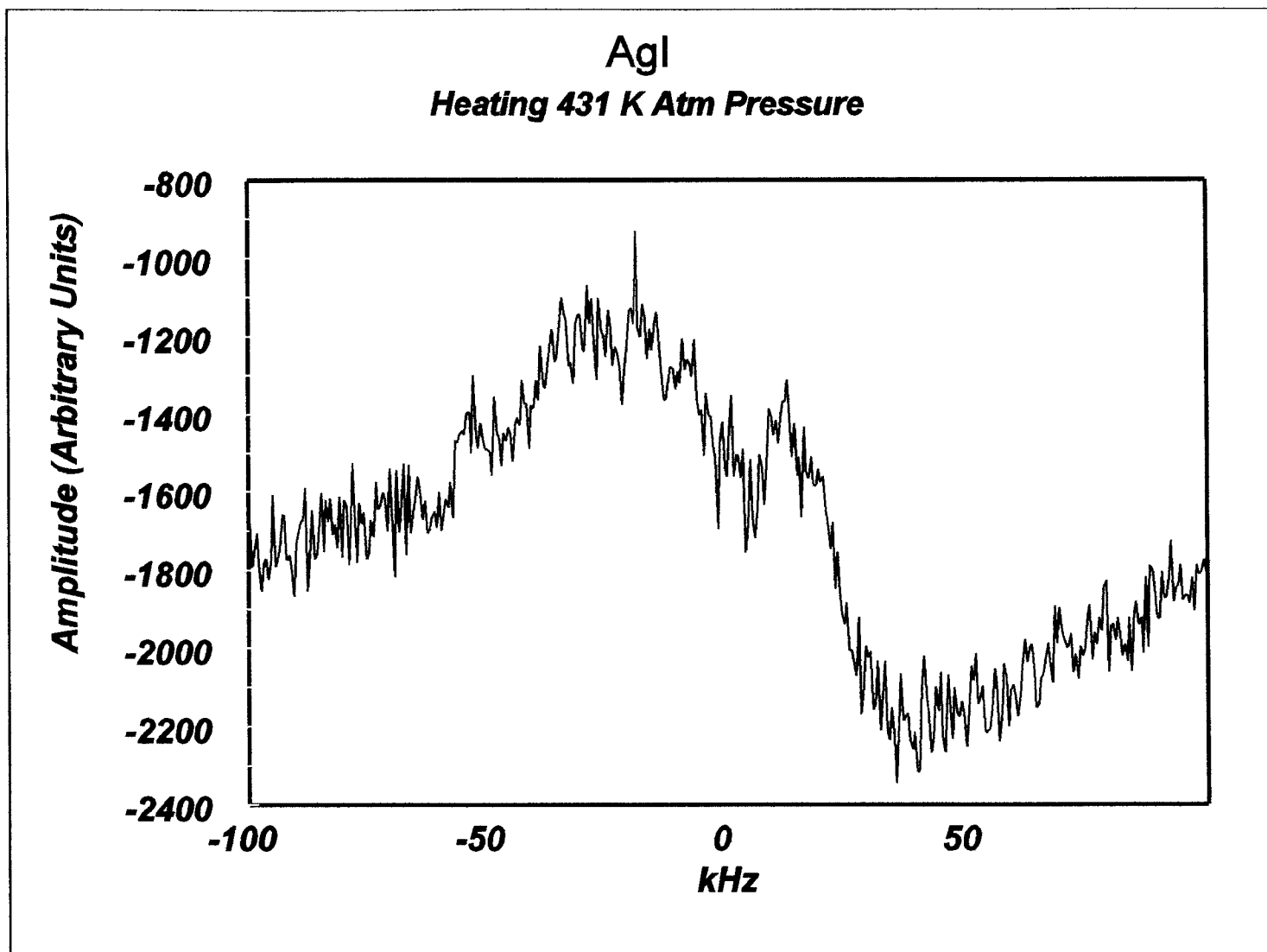


Figure 30 AgI crystal at atmospheric pressure and 431 K.

the time this spectrum was gathered. In the spectrum, gathered between 433 K and 448 K (Figure 31), no peaks are apparent near the resonant frequency indicating that the sample has undergone a phase transition and is now completely in the α phase. As the sample is cooled (Figure 32), the peaks return signalling a return to the β/γ phase.

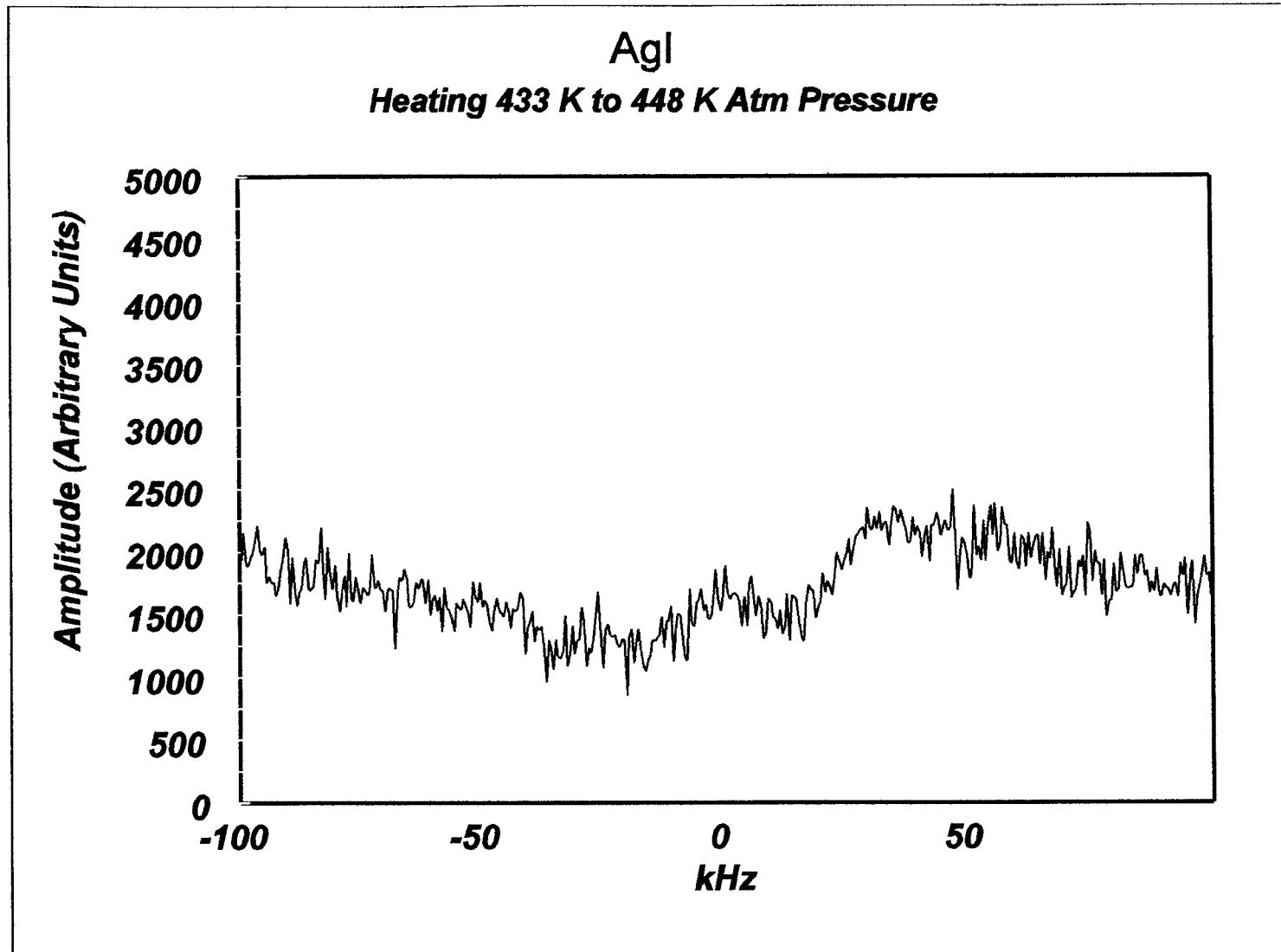


Figure 31 AgI crystal at atmospheric pressure heating from 433 K to 448 K.

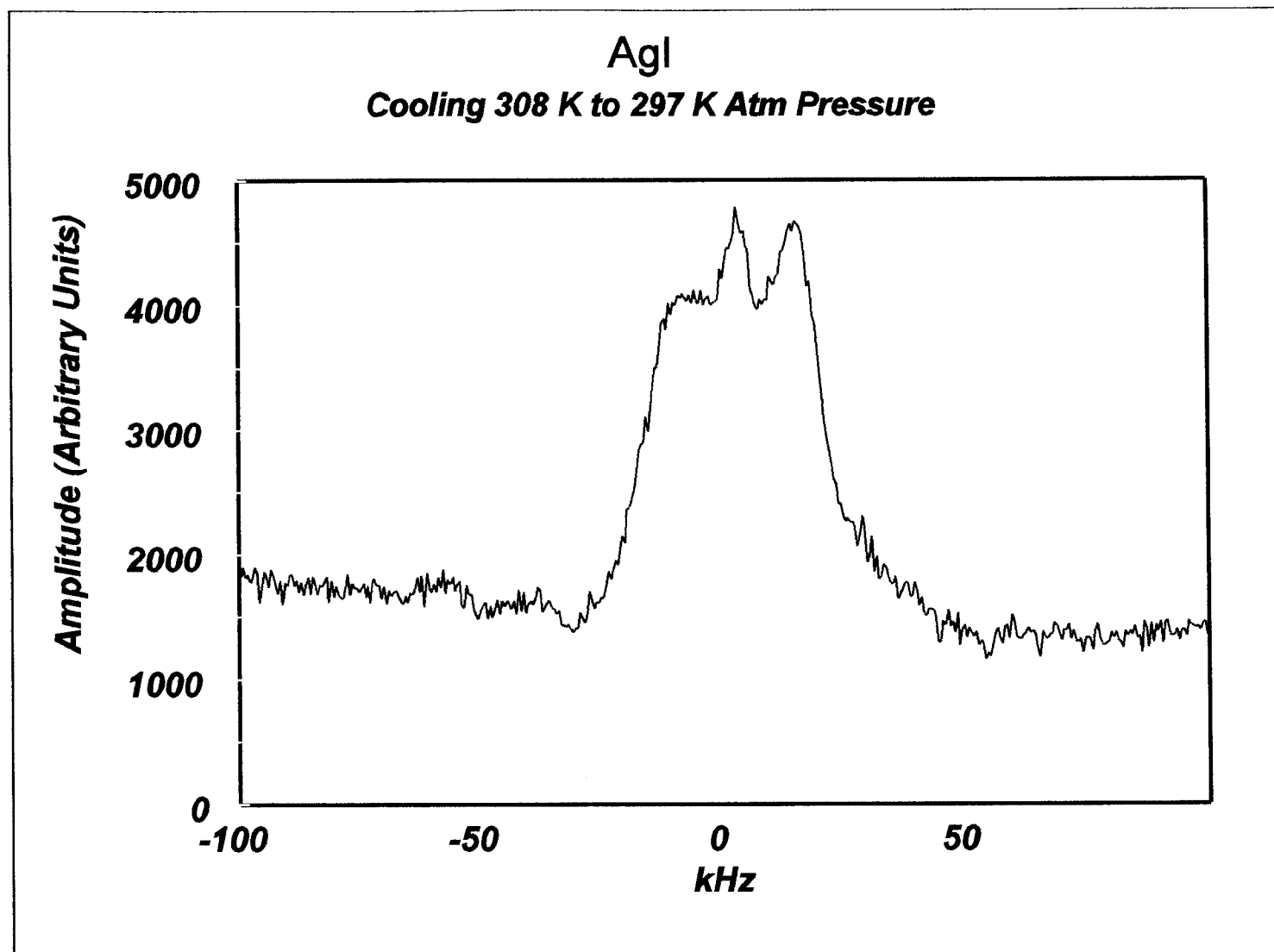


Figure 32 AgI crystal at atmospheric pressure after heating while cooling from 308 K to 297 K.

CONCLUSION

An autoclave is now available in which to perform nuclear magnetic resonance spectroscopy with internal temperatures between 273 K and 1900 K and between atmospheric pressure and 1.5 kbar. This autoclave has been successfully tested in an 8 Tesla magnet to temperatures of approximately 450 K and pressures to approximately 1.2 kbar. With suitable heaters and insulation, this autoclave should be usable in a high-field magnet at temperatures ranging to 1900 K; the autoclave is stable at these temperatures as was shown in previous work with cesium. Using this autoclave, AgI spectra have been successfully gathered at elevated temperatures and at elevated pressures. In AgI, indications of a pressure-induced transition and a temperature-induced transition have been observed.

This autoclave is currently configured for work with solid samples; however, with minor modifications, the autoclave can be configured for use with liquid samples. An existing liquid delivery system must be modified due to space constraints in the high-field spectrometer. A sample cell for use with corrosive liquids has already been designed. These modifications would allow further study of species such as liquid cesium and mercury.

BIBLIOGRAPHY

Aurora, T. S., and S. M. Day. 1982. "High-Temperature NMR Probe." *Review of Scientific Instruments* 53.8: 1152-1154.

Benedek, G. B. 1963. *Magnetic Resonance at High Pressure*. New York: Interscience Publishers.

Carter, G. C., L. H. Bennett, and D. J. Kahan. 1977. *Metallic Shifts in NMR*. Oxford: Pergamon.

El-Hanany, U. and W. W. Warren, Jr. 1975. "Knight Shift in Expanded Liquid Mercury." *Physical Review Letters* 34.20: 1276-1279.

Hoshino, H. and M. Shimoji. 1972. "The effect of the Hydrostatic Pressure on the Electrical Conductivity of Silver Iodide." *J. Phys. Chem. Solids* 33: 2303-2309.

Keen, D. A. and S. Hull. 1993. "A Powder Neutron Diffraction Study of the Pressure-Induced Phase Transitions within Silver Iodide." *Journal of Physics: Condensed Matter* 5: 23-32.

Kolem, H., O. Kanert, H. Schulz, and B. Guenther. 1990. "Design and Operation of a Variable High-Temperature Oxygen Partial-Pressure Probe Device for Solid- State NMR." *Journal of Magnetic Resonance* 87: 160-165.

Mellander, B. E. 1982. "Electrical Conductivity and Activation Volume of the Solid Electrolyte Phase α -AgI and the High-Pressure Phase fcc AgI." *Physical Review B* 26.10: 5886-5896.

Mellander, B. E., J. E. Bowling and B. Baranowski. 1980. "Phase Diagram of Silver Iodide in the Pressure Range 2.5-10 Kbar and the Temperature Range 4-330°C." *Physica Scripta* 22: 541-544.

Ploumbidis, D. 1979. "A High-Temperature and High-Field Nuclear Magnetic Resonance Instrument." *Review of Scientific Instruments* 50.9: 1133-1135.

Saito, Toshiharu, Masahiro Tatsumisago and Tsutomu Minami. 1996. "Phase Transformation and Lattice Strain of Alpha-AgI Stabilized in Superionic Glass." *Journal of the Electrochemical Society* 143: 687-691.

Sawyer, D. W. and B. N. Gale. 1973. "A Simple Sample Container for NMR Pressure and Temperature Studies on Liquids." *Journal of Physics E: Scientific Instruments* 6.

Schönherr, G., R. W. Schmutzler and F. Hensel. 1979. "Electrical and Thermodynamic Properties of Mercury in the Metal-Semiconductor Transition Range." *Philosophical Magazine B* 40.5: 411-423.

Segel, S. L., J. A. Walter, and G. J. Troup. 1969. "Quadrupole Coupling Constant of I^{127} in Hexagonal AgI." *Physica Status Solidi* 31: K43-K45.

Shaham, M. and U. El-Hanany. 1979. "A Homogeneous Very High-Temperature Minifurnace." *Journal of Physics E: Scientific Instruments* 12: 359-360.

Shimokawa, Shigezo, Hideki Maekawa, Eiji Yamada, Takashi Maekawa, Yoshio Nakamura, and Toshio Yokokawa. 1990. "A High Temperature (1200 °C) Probe for NMR Experiments and Its Application to Silicate Melts." *Chemistry Letters*: 617-620.

Stebbins, Jonathan F. 1991. "Nuclear Magnetic Resonance at High Temperature." *Chemical Review* 91: 1353-1373.

Stebbins, Jonathan F. 1992. "Nuclear Magnetic Resonance Spectroscopy of Geological Materials." *MRS Bulletin* 17.5: 45-52.

Stebbins, Jonathan F. and Ian Farnan. 1989. "Nuclear Magnetic Resonance Spectroscopy in the Earth Sciences." *Science* 245: 257-263.

Warren, W. W., Jr., G. F. Brennert and U. El-Hanany. 1989.
"NMR Investigation of the Electronic Structure of Expanded
Liquid Cesium." *Physical Review B* 39.7: 4038-4050.

Warren, W. W. and F. Hensel. 1982. "Knight Shift and
Dielectric Anomaly in Fluid Mercury." *Physical Review B*
26.10: 5980-5982.